PHYSICAL REVIEW B **84**, 224505 (2011)

Evolution of symmetry and structure of the gap in iron-based superconductors with doping and interactions

S. Maiti,[1] M. M. Korshunov,[2,3,4] T. A. Maier,[5] P. J. Hirschfeld,[2] and A. V. Chubukov[1]

[1]*Department of Physics, University of Wisconsin, Madison, Wisconsin 53706, USA*

[2]*Department of Physics, University of Florida, Gainesville, Florida 32611, USA*

[3]*L. V. Kirensky Institute of Physics, Siberian Branch of Russian Academy of Sciences, 660036 Krasnoyarsk, Russia*

[4]*Siberian Federal University, Svobodny Prospect 79, 660041 Krasnoyarsk, Russia*

[5]*Computer Science and Mathematics Division and Center for Nanophase Materials Sciences, Oak Ridge National Laboratory, Oak Ridge, Tennessee 37831, USA*

(Received 2 September 2011; revised manuscript received 11 November 2011; published 15 December 2011)

We present a detailed study of the symmetry and structure of the pairing gap in Fe-based superconductors (FeSCs). We treat FeSCs as quasi-2D, decompose the pairing interaction in the XY plane in s-wave and d-wave channels into contributions from scattering between different Fermi surfaces, and analyze how each scattering evolves with doping and input parameters. We verify that each interaction is well approximated by the lowest angular harmonics. We use this simplification to analyze the interplay between the interaction with and without spin-fluctuation components, the origin of the attraction in the $s^{\pm}$ and $d_{x^2-y^2}$ channels, the competition between them, the angular dependence of the $s^{\pm}$ gaps along the electron Fermi surface, the conditions under which the $s^{\pm}$ gap develops nodes, and the origin of superconductivity in heavily electron- or hole-doped systems, when only Fermi surfaces of one type are present. We also discuss the relation between RPA and RG approaches for FeSCs.

DOI: 10.1103/PhysRevB.84.224505 PACS number(s): 74.70.Xa, 74.20.Rp

I. INTRODUCTION

The symmetry and the structure of the superconducting gap in Fe-based superconductors (FeSCs) and their evolution and possible change with doping are currently subjects of intensive debates in the condensed-matter community. The vast majority of researchers believe that superconductivity in FeSCs is of electronic origin and results from the screened Coulomb interaction, enhanced at particular momenta due to strong magnetic fluctuations[1–13] or orbital fluctuations.[14–17] For systems with a single Fermi surface sheet, such interaction cannot lead to a simple s-wave superconductivity, but it can give rise to a superconductivity with non-s-wave symmetry: p wave for strong ferromagnetic spin fluctuations and d wave for strong antiferromagnetic spin fluctuations. In FeSCs, however, the electronic structure is more complex. The low-energy states are formed by the hybridization of all five Fe-d orbitals which in the band basis not only gives rise to multiple sheets of the Fermi surface (FS) [weakly doped FeSCs contain two electron FSs and either two or three hole FSs], but also leads to a complex mixing of contributions from intra- and interorbital terms in the interactions between low-energy fermions. In this situation, in addition to the potentially non-s-wave superconductivity, FeSCs may also develop superconductivity with an s-wave symmetry of the gap even for the repulsive electron-electron interaction. For parameters used for orbital interactions in most studies of FeSCs, the s-wave gap, averaged over the FSs, changes sign between different FS sheets (it is commonly called the $s^{\pm}$ gap), and the superconducting state competes with the spin-density-wave (SDW) state. But for other parameters, a conventional superconducting state, with a sign-preserving s^{++} gap, becomes possible, and such a state will compete with the charge-density-wave (CDW) state.[11]

The existing theoretical approaches to pairing in FeSCs can be broadly divided into two categories. One assumes that fermions at energies smaller than a fraction of the bandwidth can be treated as itinerant, with a moderate self-energy,[18] although strong coupling effects, such as interaction-driven renormalization of the whole bandwidth, have to be incorporated.[19–21] In the itinerant approach, the pairing is often treated in a BCS-Eliashberg formalism, with the interaction taken as a combination of direct electron-electron interaction and effective interaction mediated by collective bosonic excitations. Another approach assumes that the system is not far from the Mott regime and that the pairing should be affected by the tendency toward a Mott insulator.[22–24]

This work falls into the first category. Already within this category, there are several, seemingly different approaches to the pairing: the RPA-type spin-fluctuation approach (RPA-SF),[1–3,5,6,25–28] the functional RG approach (fRG),[7–9,29,30] and the analytic (logarithmic) RG approach based on a "minimal" model for the pnictides,[10–12] in which the interaction in each pairing channel is restricted to the leading angular harmonics in each pairing channel [the leading angular harmonics approximation (LAHA)]. The very positive fact for the itinerant approach as a whole is that, so far, the results of all these different approaches agree on the pairing symmetry and the gap structure in hole-doped and electron-doped FeSCs. Namely, all three approaches predict that the leading pairing instability at small to moderate dopings is in the s-wave channel, and the gap, averaged over the individual FS sheets, changes sign between hole and electron sheets (an $s^{\pm}$ gap). The $s^{\pm}$ gap generally varies along each of the FSs. If the FeSCs are treated as 2D systems (i.e., if the variation of the interaction along k_z is neglected), the variation of the gap is stronger on the electron FSs and can be large enough to create nodes. All three approaches also predict that the gap with the nodes is more likely in either undoped or electron-doped FeSCs, while in hole-doped FeSCs a no-nodal state is more likely.

The RPA and fRG formalisms have been also applied[26,30,31] to study superconductivity in recently discovered heavily electron-doped KFe_2Se_2, where only electron FSs remain,

according to recent ARPES studies.[32,33] The results of RPA-SF and fRG approaches for this limiting case are again in agreement—both predict that the gap should now have $d_{x^2-y^2}$ symmetry; i.e., it should change sign between the two electron FSs. Other approaches, however, found a conventional s-wave superconductivity in this limit, for one reason[34,35] or another.[15] A more complex sign-changing s-wave order parameter has also been suggested.[36]

The d-wave gap symmetry was also predicted by fRG[29] for heavily hole-doped KFe_2As_2, where only hole FSs are present. The RPA-SF analysis for this material[27] found attraction of comparable strength in both s-wave and d-wave channels.

The goal of this paper is to understand in more detail the evolution of the $s^{\pm}$ gap with hole and electron doping and the interplay between the $s^{\pm}$ and $d_{x^2-y^2}$ pairing in FeSCs. The idea is to "decompose" the full pairing interaction into contributions from scattering processes between different FSs and check how each process evolves with doping and input parameters. Such an analysis has been performed within the RPA-SF formalism in Ref. 1 but only for an s-wave interaction and only for a fixed doping and a particular set of input parameters.

In this work, we combine the 5-band RPA-SF and Leading Angular Harmonic Approximation (LAHA)[37] approaches. Specifically, we take the full set of interactions $\Gamma_{i,j}(\mathbf{k},\mathbf{k}')$ from the 5-band RPA-SF calculation as input (i, j label different FSs; $\mathbf{k}$ and $\mathbf{k}'$ are momenta along these FSs) and show that, for all cases that we studied, different interactions $\Gamma_{i,j}(\mathbf{k},\mathbf{k}')$ are well approximated by only two angular harmonics in s-wave and $d_{x^2-y^2}$ channels (we choose one of the momenta ($\mathbf{k}$ or $\mathbf{k}'$) such that only these two pairing channels contribute). This leaves us with a finite number of interaction parameters in each of the two pairing channels (the number of independent parameters is 4 or 5, equal to the total number of FSs). We then solve the pairing problem, obtain the eigenfunctions (which determine the gap structure) and eigenvalues (which are the dimensionless couplings), and analyze how both eigenfunctions and eigenvalues evolve with the parameters. In this work, we neglect potential new physics associated with 3D effects and treat FeSCs as quasi-2D systems, i.e., neglect the k_z dependence of the quasiparticle dispersion and of the interactions.

The key goal of our work is to understand whether superconductivity in FeSCs is governed by a single underlying pairing mechanism for all hole and electron dopings, despite that the pairing symmetry and the gap structure may change, and whether the entire variety of pairing states can be adequately described within the effective low-energy model with a small numbers of input parameters.

The specific set of issues that we address are as follows:

(1) *What is the origin of the strong angular dependence of the $s^{\pm}$ gap along the electron FSs?*

The angular dependence of the effective interaction $\Gamma_{i,j}(\mathbf{k},\mathbf{k}')$ due to the change in orbital character of the states on the FS, the competition of the scattering between hole-electron and electron-electron sheets and the local Coulomb repulsion are candidates that can give rise to a strong anisotropy of the gap.

(2) *Are the angular dependencies of all interactions relevant for the gap structure, or can some interactions be safely approximated as angle independent?*

In principle, the angular dependencies of both the electron-hole and electron-electron interactions can affect the structure of the $s^{\pm}$ gap. In the LAHA approach, we can vary the angular dependence of each interaction by hand and explore how it affects the gap structure.

(3) *Why do the $s^{\pm}$ solutions obtained within the RPA-SF and fRG approaches have nodes for systems with two hole and two electron FSs and no nodes for systems with three hole and two electron FSs? Is this behavior generic, or just a trend meaning that in both cases the $s^{\pm}$ gap is either nodal or non-nodal, depending on the input parameters?*

This issue is difficult to address in both RPA-SF and fRG approaches as these are numerical methods which require certain input parameters and exploring parameter space is computationally expensive. But it can be addressed within LAHA as one can continuously change any of the input parameters.

(4) *What causes the pairing when only electron FSs are present?*

Possibilities include pairing driven by the angular dependencies of the interactions, s-wave pairing caused by virtual scattering to gapped hole states—the "incipient" s-wave ($s^{\pm}$ gap but without hole FSs), a d-wave pairing (a plus-minus gap on electron FSs) due to magnetically enhanced repulsive interaction at momentum transfer (π,π) between the electron FSs, or an s-wave pairing if the interaction at (π,π) is strong and attractive.

(5) *What causes the pairing at large hole doping, when only hole pockets are present?*

It is possible that the scattering between hole FSs with wave vector (π,π) favors $s^{\pm}$ pairing while the alternative is that Coulomb avoidance within each FS pocket makes nodal d wave the preferable symmetry.

(6) *How is the structure of the pairing interaction affected when the spin-fluctuation component is added to the direct fermion-fermion interaction?*

Inclusion of the SF contribution can affect the relative magnitudes of the interactions $\Gamma_{ij}(\mathbf{k},\mathbf{k}')$ between different FS sheets and in principle can change its angular dependence.

This last issue is relevant for understanding the comparison between RPA-SF and RG approaches, which we pause to discuss in some detail. These two approaches differ in the assumption of what are the relevant energy scales for magnetism and superconductivity. In the RG approach it is assumed that magnetism and superconductivity are produced by the same low-energy fermions and have to be treated on equal footing, starting from a model with only density-density and exchange interaction between fermions. Then the SF component of the interaction develops together with the pairing vertex (one builds up step-by-step "parquet" renormalizations simultaneously in the particle-hole and particle-particle channels).[7,11,12] In the RPA-SF approach[2,5,6,25] the assumption is that magnetism is superior to superconductivity and comes from fermions at energies comparable to the bandwidth, which are above the upper edge for the RG treatment. If so, the SF component should be included into the bare interaction, which does not need to be further renormalized in the particle-hole channel. In this situation, only renormalizations in the particle-particle channel (which always come from low-energy fermions) remain relevant, and the RG treatment becomes equivalent to the BCS theory. There is no good justification to select a particular set of diagrams for the renormalization

of the interaction at high energies, but in many cases the RPA approximation (which amounts to a summation of ladder series of vertex renormalization diagrams in the spin channel and generally accounts for a Stoner-type instability at some Q) yields quite reasonable effective interactions, particularly near a magnetic instability.

Which of the two approaches better describes FeSCs is debatable. The value of the ordered magnetic moment is quite small, at least in the FeSCs, and magnetic excitations measured by neutron scattering die off at energies of 100–150 meV. This behavior is consistent with the idea that magnetism comes from relatively low-energy fermions. The one-loop parquet RG equations for the coupled flow of the vertices are rigorously justified only when the fermionic dispersion can be approximated by a k^2 dependence. This also does not extend too far in energy; i.e., the upper limit for the RG approach is also only a fraction of the bandwidth.

But are these two approaches fundamentally different? To compare them, we remind the reader that in the RG treatment, the flow of magnetic and superconducting vertices remain coupled only down to energies of order E_F. At energies $E < E_F$, each vertex flows independently, and the flow of the pairing vertex (Γ_{sc}) becomes the same as in the BCS theory ($d\Gamma_{sc}/d\log E = \Gamma_{sc}^2$. From this perspective, the real result of RG as far as pairing is concerned is the renormalization of the pairing interaction from its bare value to the renormalized one at E_F. [This is indeed only true if the RG flow does not reach a fixed point down to E_F, but this is likely to be the case for FeSCs simply because T_c and T_N are both small compared to $E_F \sim 0.1$ eV.] It is quite likely (although not guaranteed) that the angle-independent components of the renormalized interactions can be reproduced by choosing some other input parameters in the orbital basis; i.e., the effect of the RG flow could be absorbed into the modification of the bare theory. The same is true for the RPA-SF approach—the angle-independent components of the new SF interactions likely can be reproduced the renormalization of input parameters, although the needed values of U, V, J, J' may seem quite exotic.

The situation is a bit more tricky for the angle dependent components of the interactions. The RG with coupled magnetic and superconducting vertices can be rigorously justified at weak coupling only if angular dependence of the vertices are (i) weak and (ii) are preserved under RG. This is how the analytic RG flow has been obtained.[12] fRG does include some variation of the angle dependence of interactions, but this goes beyond justifiable logarithmic accuracy. Given that fRG and analytic RG yield virtually identical results, it seems as if the only effect of RG renormalizations down to E_F is the rescaling of the overall magnitudes of the interactions. If the effect of adding the SF component to the interaction in the RPA-SF approach also predominantly gives rise to rescaling of the magnitudes of the interactions, then the two approaches are not fundamentally different.

This does not imply that the RPA-SF and RG approaches are equivalent. Rather, the implication is that the outcome of applying each of the two formalisms is the new "bare" theory with new input parameters. These new parameters do differ somewhat between RPA-SF and RG, but the difference should not matter much if the pairing symmetry and the gap structure are quite robust with respect to parameter variations. This is another issue that one can straightforwardly verify using the LAHA formalism which allows one to continuously change the parameters.

This paper is organized as follows. In Sec. II we briefly discuss the RPA-SF and LAHA formalisms and outline the computational procedure. In Sec. III we discuss how the gap symmetry and structure are affected by the SF component of the interaction. In Sec. IV we show the results for weakly electron-doped and hole-doped FeSCs, and in Sec. V we discuss strongly electron- and hole-doped FeSCs, which contain only electron or hole pockets, respectively. We present our conclusions in Sec. VI. A short summary of this work is presented in Ref. 37.

II. THE RPA-SF AND LAHA FORMALISMS AND THE COMPUTATIONAL PROCEDURE

We first briefly describe the RPA-SF and LAHA approaches and then outline the computational procedure.

A. RPA-SF formalism

The approach and its application to FeSCs have been discussed in detail in several recent publications,[2,5,6] so we will be brief. The point of departure for RPA-SF is a 5-orbital model with intraorbital and interorbital hopping integrals and density-density (Hubbard) and exchange intraorbital and interorbital interactions given by

$$H_{\rm int} = U\sum_{f,s} n_{f,s\uparrow}n_{f,s\downarrow} + \sum_{f,s,t\neq s}\left(\frac{V}{2}n_{fs}n_{ft} - \frac{J}{2}\vec{S}_{fs}\cdot\vec{S}_{ft}\right) + \frac{J'}{2}\sum_{f,s,t\neq s}\sum_{\sigma} c^{\dagger}_{fs\sigma}c^{\dagger}_{fs\bar{\sigma}}c_{ft\bar{\sigma}}c_{ft\sigma}, \quad (1)$$

where $c_{fs\sigma}$ is the annihilation operator for electron on lattice site f with orbital index s and spin σ, $n_{fs} = n_{f,s\uparrow} + n_{f,s\downarrow}$, $n_{fs\sigma} = c^{\dagger}_{fs\sigma}c_{fs\sigma}$ is the density operator, $\vec{S}_{fs} = (1/2)c^{\dagger}_{fs\alpha}\vec{\sigma}_{\alpha\beta}c_{fs\beta}$ is the spin operator, and $\bar{\sigma} = -\sigma$. We have designated different symbols for the intraorbital Coulomb interaction U, interorbital Coulomb interaction V, interorbital exchange J, and "pair hopping" term J' for generality, but note that if they are generated from a single spin-rotational-invariant two-body term they are related by $J' = J/2$ and $V = U - 5J/4$. The model parameters for hopping integrals (36 total) are obtained from the fit to density functional theory (DFT) band structure,[38] see Ref. 2 for detailed description of the model parameters.

The SF component of the interaction is now obtained by summing up second- and higher-order ladder diagrams in matrix orbital formalism. The total interaction (the sum of the direct, first-order term and SF contribution) is then converted from orbital to band basis by dressing it by matrix elements associated with the hybridization of five Fe orbitals. The end result of this procedure for the purposes of the analysis of superconductivity is the effective BCS-type Hamiltonian in the band description

$$\mathcal{H} = \sum_{i,\mathbf{k}}\epsilon_i(\mathbf{k})c^{\dagger}_{i\mathbf{k}}c_{i\mathbf{k}} + \sum_{i,j,\mathbf{k},\mathbf{k}'}\Gamma_{ij}(\mathbf{k},\mathbf{k}')c^{\dagger}_{i\mathbf{k}}c^{\dagger}_{i-\mathbf{k}}c_{j\mathbf{k}'}c_{j-\mathbf{k}'}. \quad (2)$$

The quadratic term describes low-energy excitations near hole and electron FSs, labeled by i and j, and the interaction term describes the scattering of a pair $(k\uparrow, -k\downarrow)$ on the FS i to a pair $(-k'\uparrow, k'\downarrow)$ on the FS j. The effective singlet interaction $\Gamma_{ij}(\mathbf{k},\mathbf{k}')$ is then given by

$$\Gamma_{ij}(\mathbf{k},\mathbf{k}') = \sum_{s,t,p,q} \mathrm{Re}\left[a^{t*}_{\nu_i}(-\mathbf{k})a^{s*}_{\nu_i}(\mathbf{k})\Gamma st^{pq}(\mathbf{k},\mathbf{k}',0)a^{p}_{\nu_j}(\mathbf{k}')a^{q}_{\nu_j}(-\mathbf{k}')\right], \tag{3}$$

with

$$\Gamma^{pq}_{st}(\mathbf{k},\mathbf{k}',\omega) = \left[\tfrac{1}{2}U^s + \tfrac{1}{2}U^c + \tfrac{3}{2}U^s\chi_1^{\mathrm{RPA}}(\mathbf{k}-\mathbf{k}',\omega)U^s - \tfrac{1}{2}U^c\chi_0^{\mathrm{RPA}}(\mathbf{k}-\mathbf{k}',\omega)U^c\right]^{tq}_{\mathrm{ps}}. \tag{4}$$

Here the χ_1^{RPA} and χ_0^{RPA} describe the spin fluctuation contribution and orbital (charge) fluctuation contribution, respectively, $a^p_{\nu_j}$ is the matrix element connecting orbital p with the band ν_j on FS j, and the matrices U^c and U^s contain interaction parameters from Eq. (1) as described in Ref. 2. We will call an approximation to the total interaction which includes only the two first-order terms in Eq. (4) as "constant or non-spin-fluctuation" (NSF), while the total interaction includes the third and fourth spin-fluctuation terms (SF) as well. In principle this interaction includes also charge (orbital) fluctuations via U^c, but as these are negligible for realistic parameters, we use the simpler "spin fluctuation" designation.

Throughout this paper, we consider the pairing in the unfolded Brillouin zone, leaving aside the issue of possible changes of the gap due to folding. These are particularly important in the case of the 122 systems with $I4/mmm$ symmetry.[14,36] In the unfolded zone, the 2D electronic structure of weakly and moderately electron-doped FeSCs consists of two near-circular FSs centered at Γ point ($\mathbf{k}=0$) and two elliptical electron FSs centered at X and Y points, $\mathbf{k}=(0,\pi)$ and $\mathbf{k}=(\pi,0)$, respectively. For hole-doped and some undoped FeSCs, there exists also another, third, hole FS located at M point $\mathbf{k}=(\pi,\pi)$. In the folded zone, all three hole FSs are centered at (0,0), and the two electron FSs move to (π,π) and are hybridized through the coupling via a pnictogen.

The interaction $\Gamma_{ij}(\mathbf{k},\mathbf{k}')$ contains all pairing components for tetragonal (D_{4h}) lattice symmetry: A_{1g} (s wave), B_{1g} ($d_{x^2-y^2}$), B_{2g} (d_{xy}), and A_{2g} (g wave). The s-wave gap $\Delta_s(k_x,k_y)$ is symmetric under $k_x \to \pm k_x, k_y$, the $d_{x^2-y^2}$ gap $\Delta_{d_{x^2-y^2}}(k_x,k_y)$ changes sign under $k_x \to k_y$, and so on. We focus here on s- and $d_{x^2-y^2}$-wave symmetries.

With these considerations in mind, the BCS gap equation then becomes the eigenvalue problem:

$$\sum_j \oint_{C_j} \frac{dk'_\parallel}{2\pi}\frac{1}{2\pi v_F(\mathbf{k}'_F)}\Gamma_{ij}(\mathbf{k}_F,\mathbf{k}'_F)\Delta_{\alpha,j}(\mathbf{k}'_F)L = -\lambda_\alpha\Delta_{\alpha,i}(\mathbf{k}_F), \tag{5}$$

where α is either s or $d_{x^2-y^2}$ and $L \sim \ln(E_F/T_c)$. For a circular FS, Eq. (5) is simplified to

$$\sum_j \int_0^{2\pi} \frac{d\psi'}{2\pi} N_{F,j}\Gamma_{ij}(\psi,\psi')\Delta_{\alpha,j}(\psi')L = -\lambda_\alpha\Delta_{\alpha,i}(\psi), \tag{6}$$

where $N_{F,j} = m_j/2\pi$ is the density of states at the FS j, and ψ and ψ' are the angles along the FSs i and j, respectively.

Equations (5) and (6) are integral equations which in general can be solved only numerically. Taking M points on each FS, one obtains M eigenfunctions and M different λ's in each of the two pairing channels. For s wave, some of eigenfunctions correspond to an s^{++} gap, while others correspond to an $s^{\pm}$ gap. The eigenfunction corresponding to the largest positive λ_α describes the pairing state immediately below T_c.

B. LAHA formalism

The generic idea of LAHA approximation is to model $\Gamma_{ij}(\mathbf{k},\mathbf{k}')$ by a rather simple function of the two momenta, such that the gap equation can be solved *and analyzed* analytically. In cuprates, numerous groups approximated the $d_{x^2-y^2}$ gap by the first harmonic $\cos k_x - \cos k_y$ ($\cos 2\phi$ for a circular FS) and neglected higher harmonics such as $\cos 6\phi$, $\cos 10\phi$, etc. The smallness of $\cos(4n+2)\phi$ terms with $n \geqslant 1$ does not follow from any underlying principle, but numerically the $\cos 2\phi$ approximation works rather well, at least at and above optimal doping.

Such an approximation should generally work even better for FeSCs because all FSs are small and even electron ones are almost circular. By analogy with the cuprates, one may try to approximate s-wave eigenfunction by a constant along each FS, and approximate $d_{x^2-y^2}$ gaps by $\cos 2\phi$. There is a caveat, however—such approximation is only valid for the gaps along hole FSs which are centered at the points along $k_x = \pm k_y$ [i.e., at $k=(0,0)$ and $(\pm\pi, \pm\pi)$]. Electron FSs are centered at X and Y points, which by itself are not $k_x \to \pm k_y$ symmetric. As a result, some of the s-wave gap functions, such as $\cos k_x + \cos k_y$, behave as $\pm\cos 2\theta$, where θ is the angle along an electron FS, while some of the d-wave gap functions such as $\cos k_x - \cos k_y$ are approximated by constants on the two electron FSs. In the latter case, the only "memory" about the d-wave is that the sign of a constant changes between the two electron FSs.

The implication of this result is that, within LAHA, angle-independent and $\cos 2\theta$ terms must appear together in both s-wave and d-wave components of the interactions, and with comparable magnitudes. A simple analysis then shows that the form of the interaction depends on whether it involves hole or electron FSs. For the interaction between fermions on a hole FS, in LAHA,

$$\Gamma_{hh}(\phi,\phi') = A_{hh} + \tilde{A}_{hh}\cos 2\phi\cos 2\phi', \tag{7}$$

where ϕ and ϕ' are the angles along a hole FS (measured relative to the k_x axis), and the A and $\tilde{A}$ terms are s-wave and d-wave components, respectively. For the interaction between fermions from a hole and an electron FS,

$$\Gamma_{eh}(\phi,\theta) = A_{eh}\,(1+2\alpha\cos 2\theta) + \tilde{A}_{eh}\cos 2\phi\,(1+2\tilde{\alpha}\cos 2\theta), \tag{8}$$

where θ is the angle along an electron FS (again, measured relative to the k_x axis). Finally, for the interaction between fermions from an electron FS, we have in

LAHA

$$\Gamma_{ee}(\theta,\theta') = A_{ee}[1+2\alpha(\cos 2\theta+\cos 2\theta')+4\beta\cos 2\theta\cos 2\theta'] + \tilde{A}_{ee}[1+2\tilde{\alpha}(\cos 2\theta+\cos 2\theta')+4\tilde{\beta}\cos 2\theta\cos 2\theta']. \tag{9}$$

The s-wave and d-wave components look identical, but they transform differently between intra- and interpocket interactions involving the electron FSs.

Below we present the full LAHA result for $\Gamma_{ij}(\mathbf{k}_F,\mathbf{k}'_F)$ for the case when the FS consists of two hole and two electron pockets. The extension to the case of three hole FSs is straightforward. We have

$$\begin{aligned}
\Gamma_{h_ih_j}(\phi,\phi') &= U_{h_ih_j}+\tilde{U}_{h_ih_j}\cos 2\phi\cos 2\phi',\\
\Gamma_{h_ie_j}(\phi,\theta) &= U_{h_ie}\big(1\pm 2\alpha_{h_ie}\cos 2\theta\big)+\tilde{U}_{h_ie}\big(\pm 1\\
&\quad +2\tilde{\alpha}_{h_1e}\cos 2\theta\big)\cos 2\phi,\\
\Gamma_{e_ie_i}(\theta,\theta') &= U_{ee}[1\pm 2\alpha_{ee}(\cos 2\theta+\cos 2\theta')\\
&\quad +4\beta_{ee}\cos 2\theta\cos 2\theta']+\tilde{U}_{ee}[1\pm 2\tilde{\alpha}_{ee}\\
&\quad \times(\cos 2\theta+\cos 2\theta')+4\tilde{\beta}_{ee}\cos 2\theta\cos 2\theta'],\\
\Gamma_{e_1e_2}(\theta,\theta') &= U_{ee}[1+2\alpha_{ee}(\cos 2\theta-\cos 2\theta')\\
&\quad -4\beta_{ee}\cos 2\theta\cos 2\theta']+\tilde{U}_{ee}[-1-2\tilde{\alpha}_{ee}\\
&\quad \times(\cos 2\theta-\cos 2\theta')+4\tilde{\beta}_{ee}\cos 2\theta\cos 2\theta'],
\end{aligned} \tag{10}$$

where the upper sign is for the electron pocket e_1 and the lower sign is for e_2; $i,j\in 1,2$. Intrapocket s-wave components $U_{h_ih_i}$ and U_{ee} represent the total strength of intra- and interorbital Coulomb (Hubbard) interaction and are positive (repulsive). The signs of U_{h_ie} are determined by the relative magnitudes of intraorbital U and interorbital V terms. For a toy model of two orbitals which hybridize to give one hole and one electron band, $U_{he}>0$ if intraorbital Hubbard repulsion U exceeds interorbital V, and $U_{he}<0$ for $V>U$.[11] It is generally expected that the intraorbital interaction is the largest, and below we assume that U_{he} is positive. If, however, $V>U$, the interaction between electrons and holes is attractive in which case it favors a conventional s-wave superconductivity.[14] The signs of d-wave components of the interactions are determined by a more subtle balance between different U's and J's.

Later in the text we will use instead of U_{ij} dimensionless interactions:

$$u_{ij}=U_{ij}(N_{F,i}N_{F,j})^{1/2}. \tag{11}$$

The equation for Δ_{α_i} and λ_α is the same as Eq. (6). However, now we do not have to solve the integral equation on the gap because for Γ_{ij} given by Eq. (10), s-wave and d-wave gaps have only four components each. For the case of two hole pockets the s-wave gap is of the form

$$\begin{aligned}
\Delta_{h_1}(\phi)=\Delta_{h_1},\Delta_{e_1}(\theta)=\Delta_e+\bar{\Delta}_e\cos 2\theta,\\
\Delta_{h_2}(\phi)=\Delta_{h_2},\Delta_{e_2}(\theta)=\Delta_e-\bar{\Delta}_e\cos 2\theta,
\end{aligned} \tag{12}$$

and the d-wave gap is of the form

$$\begin{aligned}
\Delta_{h_1}(\phi)=\Delta_{h_1}\cos 2\phi,\Delta_{e_1}(\theta)=\Delta_e+\bar{\Delta}_e\cos 2\theta,\\
\Delta_{h_2}(\phi)=\Delta_{h_2}\cos 2\phi,\Delta_{e_2}(\theta)=-\Delta_e+\bar{\Delta}_e\cos 2\theta.
\end{aligned} \tag{13}$$

To obtain λ_α and eigenfunctions we need to write down and diagonalize 4×4 matrix gap equations.[39] The equations on λ_s and λ_d are fourth-order algebraic equations; hence there are effectively only four parameters which determine the couplings and the gap structure in each channel. This is the same number as the minimal number of interaction parameters in the original orbital model.

The situation becomes even more simple if the two hole FSs can be treated as equal (i.e., $u_{h_ih_j}=u_{hh}$, $u_{h_1e}=u_{h_2e}=u_{he}$, and $\alpha_{h_1e}=\alpha_{h_2e}=\alpha$, which actually is quite consistent with the fits to RPA-SF; see below). Then $\Delta_{h_1}=\Delta_{h_2}=\Delta_h$ and the gap equation reduces to a 3×3 set which can be very easily analyzed analytically. For the s-wave gap, the 3×3 matrix is

$$\begin{pmatrix} 1+2u_{hh}L & 2u_{he}L & 2\alpha_{he}u_{he}L\\ 2u_{he}L & 1+2u_{ee}L & 2\alpha_{ee}u_{ee}L\\ 4\alpha_{he}u_{he}L & 4\alpha_{ee}u_{ee}L & 1+4\beta_{ee}u_{ee}L \end{pmatrix}, \tag{14}$$

and for the d-wave gap it is

$$\begin{pmatrix} 1+\tilde{u}_{hh}L & 2\tilde{u}_{he}L & 2\tilde{\alpha}_{he}\tilde{u}_{he}L\\ \tilde{u}_{he}L & 1+2u_{ee}L & 2\tilde{\alpha}_{ee}\tilde{u}_{ee}L\\ 2\tilde{\alpha}_{he}\tilde{u}_{he}L & 4\tilde{\alpha}_{ee}\tilde{u}_{ee}L & 1+4\tilde{\beta}_{ee}\tilde{u}_{ee}L \end{pmatrix}. \tag{15}$$

The eigenvalues λ_s and λ_d (three of each) and the corresponding eigenfunctions are obtained by diagonalizing this matrix equation and casting the result as $\mathrm{diag}(1-\lambda_\alpha L)$.

For the case of three hole FSs, we have to introduce three different Δ_{h_i}. The gap equations in the s-wave and d-wave channels become 5×5 sets. Still, they can be very easily analyzed.

C. General considerations

Before we proceed further, it is instructive to take a more careful look at the 3×3 sets Eqs. (14) and (15) to illustrate issues which we outlined in the introduction. Consider first the s-wave gap equation. Suppose momentarily that all interactions are angle independent; i.e., α_{he}, α_{ee}, and $\beta_{ee}=0$. Then we have three solutions:

$$\lambda_s=\begin{cases} 0,\\ -\frac{u_{hh}+u_{ee}}{2}-\sqrt{\left(\frac{u_{hh}-u_{ee}}{2}\right)^2+u_{he}^2},\\ -\frac{u_{hh}+u_{ee}}{2}+\sqrt{\left(\frac{u_{hh}-u_{ee}}{2}\right)^2+u_{he}^2}. \end{cases} \tag{16}$$

A positive (attractive) λ_s emerges only when $u_{eh}^2>u_{ee}u_{hh}$, i.e., when the interpocket pair hopping interaction term exceeds intrapocket repulsion. The eigenfunction corresponding to the positive λ_s is a sign-changing $s^{\pm}$ gap: $\Delta_e=-\Delta_h$. The one corresponding to the negative λ_s is a conventional s^{++} gap: $\Delta_e=\Delta_h$.

Suppose next that the angular dependence of the interaction is present. Then $\pm\cos 2\theta$ components of the gaps along electron FSs become nonzero. Solving the cubic equation for λ_s, we now find three nonzero solutions. When $u_{eh}^2>u_{ee}u_{hh}$, the solution with the largest λ_s gradually evolves from the one which already existed for constant interactions. When α_{he}, α_{ee}, and β_{ee} increase, the $\cos 2\theta$ component of $\bar{\Delta}_e$ grows, and at some point becomes larger than Δ_e, and the gap develops nodes. This is one scenario. Another one comes from the analysis of the region $u_{eh}^2<u_{ee}u_{hh}$, where no $s^{\pm}$ solution was

possible without angular dependence of the interactions. In that case, one of λ_s was zero. When the angular dependence is included, this λ_s becomes nonzero, and its sign is determined by the sign of

$$S = u_{ee}u_{hh}\left(\alpha_{ee}^2 - \beta_{ee}\right) + u_{eh}^2\left(\alpha_{eh}^2 + \beta_{ee} - 2\alpha_{ee}\alpha_{eh}\right). \quad (17)$$

When $S > 0$, $\lambda_s > 0$; i.e., the system develops an attraction in the s-wave channel exclusively because of the angular dependence of the interactions. The eigenfunction corresponding to such λ_s has nodes even when the angular dependence of the interactions is weak. The physics picture is that the system finds a way to minimize the effect of strong intrapocket repulsion u_{ee} by inflating $\cos 2\theta$ components of the gaps along the electron FSs, because these components do not couple to the angle-independent component of the interaction.

Note that the sign of S is predominantly determined by the interplay between the angular dependence of electron-hole and electron-electron interactions. When $\alpha_{eh} \gg \alpha_{ee}$, or when $\alpha_{ee}^2 > \beta_{ee}$, $S > 0$ even when $u_{ee}u_{hh} \gg u_{eh}^2$; i.e., $s^{\pm}$ superconductivity with nodes develops despite the fact that intrapocket repulsion is the strongest. In particular, S is definitely positive if only electron-hole interaction has momentum dependence, i.e., if $\alpha_{ee} = \beta_{ee} = 0$. In this situation, $S = u_{eh}^2\alpha_{eh}^2 > 0$.

Consider next the limit when hole FSs are absent and only electron ones are present. At first thought, s-wave pairing is impossible. On a more careful look, however, we find from Eq. (14) that, even if we set $u_{eh} = 0$, one of λ_s for s-wave pairing is still positive if $\beta_{ee} < \alpha_{ee}^2$, no matter how small angular dependence of electron-electron interaction is. The eigenfunction for this solution again has nodes. The physics reasoning is the same as in the case we just considered: The angle-independent part of the interaction is repulsive, but the system finds a way to overcome this strong repulsion by inflating $\cos 2\theta$ components of the gaps along the electron FSs.

We next turn to the d-wave gap equation Eq. (15). The generic reasoning parallels the one for the s-wave case. Namely, for interactions independent of $\cos 2\theta$, the attractive d-wave solution exists when $\tilde{u}_{eh}^2 > \tilde{u}_{ee}\tilde{u}_{hh}$, and for angle-dependent interaction one of λ_d is positive (attractive) even if this condition is not satisfied, but $\tilde{S}$, which is a d-wave analog of S from Eq. (17), is positive. There is, however, one crucial distinction with the s-wave case: The d-wave interactions $\tilde{u}_{hh}$ and $\tilde{u}_{ee}$ are not necessary positive. In particular, $\tilde{u}_{ee}$ is the difference between angle-independent components of intrapocket and interpocket interactions between electron pockets. Once the interpocket interaction is larger [e.g., when magnetic fluctuations are peaked at (π,π)], $\tilde{u}_{ee} < 0$, and the system develops an attraction in the d-wave channel, even when d-wave electron-hole interaction is weak. This is particularly relevant for the case when only electron FSs are present; i.e., within the BCS approximation $\tilde{u}_{eh}$ can be set to zero. If $\tilde{u}_{ee} < 0$ in this case, the d-wave solution emerges, with the sign-changing gap on the two electron FSs. An alternative possibility is that $\tilde{u}_{ee} > 0$ but $\tilde{\alpha}_{ee}^2 > \tilde{\beta}_{ee}$, and the d-wave attraction is produced by the angle-dependent part of the d-wave interaction. In this situation, the $\cos 2\theta$ component of the d-wave gap is large, and the gap has nodes on the two electron FSs.

TABLE I. Six sets of parameters used in comparison of RPA-SF and LAHA. We used different values of the chemical potential μ for each set ($\mu = -0.20$ to $+0.30$); the range covers hole doping (negative) to electron doping (positive). All parameters in this text are in eV.

Set	U	J	V
1	1.67	0.21	1.46
2	1.0	0.25	0.69
3	1.2	0.0	1.2
4	1.0	0.9	−1.25
5	1.0	4.0	−4.0
6	1.0	0.9	−0.7

D. Computational procedure

We use $\Gamma_{ij}(\mathbf{k}_F,\mathbf{k}'_F)$ obtained in the RPA-SF approach as inputs and fit their functional forms by Eq. (10). This gives us U_{ij}, α_{ij}, and β_{ij}. We assume for simplicity that $N_{F,j}$ are the same for all FSs, convert U_{ij} into $u_{ij} = N_F U_{ij}$, and analyze 4×4 and 5×5 gap equations. We then vary parameters and check how robust the solutions are. The approach can be extended to the case when $N_{F,j}$ depends on j, but this dependence very likely does not change the physics.

We analyzed six different sets of parameters and several different doping levels which correspond to either electron doping or hole doping. The parameters are presented in Table I. The results for all sets of parameters are quite similar, and below we show the results only for representative cases. We also analyze the case of large electron doping, when there are no hole FSs.

The use of LAHA is meaningful only if the fit of the actual $\Gamma_{ij}(\mathbf{k}_F,\mathbf{k}'_F)$ by Eq. (10) is accurate enough. In Figs. 1 and 2 we show fits for the representative case of $\mu = 0.08$ (electron doping with $n_e = 6.12$, while the undoped case is $n_e = 6$) and interactions from set 1 ($U = 1.67$, $J = J' = 0.21$, $V = 1.41$) considered in Ref. 1. n_e is the number of electrons per Fe atom. It is equal to 6 for the undoped case and >6 (<6) for the electron (hole) doping. We set one of momenta to be either along the x or along the y axis on one of the four FSs and vary the other momentum along all four FSs. The parameters for the s-wave and d-wave interactions extracted from the fit are presented in Table II.

The original $\Gamma_{ij}(\mathbf{k}_F,\mathbf{k}'_F)$ are in the units of eV. Within our approximation of an equal $N_{F,j}$ on all FSs, the dimensionless u_{ij} are $\Gamma_{ij}(\mathbf{k}_F,\mathbf{k}'_F)$ times the rescaling factor. This factor affects the overall scale of the eigenvalues λ but does not affect the sign and relative magnitudes of λ_s and λ_d, which we need. For simplicity, we then set this rescaling factor to be equal to 1.

We see that the fits are reasonably good. For the case of no SF term (NSF), all $\Gamma_{ij}(\mathbf{k}_F,\mathbf{k}'_F)$ are fitted well by Eq. (10). For the full interaction (i.e., SF included), all $\Gamma_{ij}(\mathbf{k}_F,\mathbf{k}'_F)$ are fitted well, and the discrepancies can be cured by including subleading $\cos 4\theta$ terms into the interactions.

The fits for other parameters are quite similar. For example in Figs. 7–9 below we show the best and the worst fits of interactions for set 2 for three different values of μ. For positive μ, there are four FSs, and for negative μ, there is an additional, fifth hole FS. The fits are not perfect, but are quite good for all practical purposes.

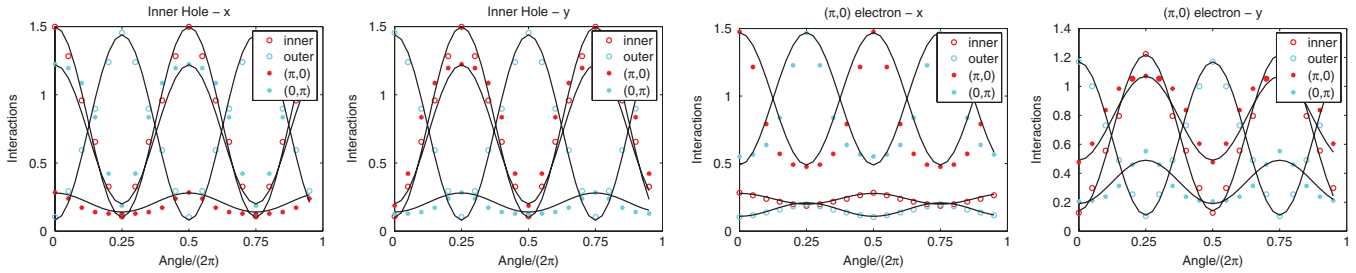

FIG. 1. (Color online) Fits of the actual interactions $\Gamma_{ij}(\mathbf{k}_F,\mathbf{k}'_F)$ by LAHA. Symbols represent interactions computed numerically for the 5-orbital model using LDA band structure; solid lines are fits using Eq. (10). The fit is for set 1 for bare interactions (no SF component). The chemical potential is $\mu = 0.08$ which corresponds to electron doping. We set $\mathbf{k}_F$ in $\Gamma_{ij}(\mathbf{k}_F,\mathbf{k}'_F)$ to be either along the x or along the y direction on a given FS (its location is specified in the title on top of each figure) and varied $\mathbf{k}'_F$ along each of the FSs. The angle θ' is measured relative to k_x. The fit is reasonably good.

One can quantify the accuracy of LAHA by looking at the contributions from the higher harmonics. We compare the strength of leading and subleading angular harmonics in the s and d channels in Table III. We clearly see that the subleading harmonics are smaller than the leading terms, which, we remind the reader, are constant *or* $\cos 2\phi$ terms for hole-hole interactions in the s- and d-wave channels, respectively, and constant *and* $\cos 2\theta$ terms for hole-electron interaction, when we vary the angle along the electron FS.

We continue below with set 1 for the discussion on how the SF contribution affects the pairing symmetry and the gap structure. The trend is the same for all other sets. And just for a change we will look at set 2 for the discussion of how gap symmetry and structure change with doping. We do so to limit the number of figures and not overwhelm the reader. We will point out in the text if differences arise.

III. SENSITIVITY OF THE GAP STRUCTURE TO THE FORM OF $\Gamma_{ij}(\mathbf{k}_F,\mathbf{k}'_F)$

We first use the parameters extracted from the fit for set 1 and solve the 4×4 gap equation within LAHA. The results for the case of no SF component are shown in Fig. 3. For comparison, the gaps obtained by the full numerical solution within RPA are also presented. The LAHA and RPA solutions are almost equivalent, which is another indication that the LAHA fit works quite well. The results for the full interaction, with the SF component, are also presented in Fig. 3 along with the numerical solution for s-wave gap within RPA-SF. The LAHA and RPA solutions again agree very well. The only real difference between RPA-SF and LAHA is that the value of the gap along the outer hole FS is somewhat larger in RPA-SF. As we said, this is a consequence of the fact that to fit $\Gamma_{h_2,e}(\phi,\theta)$ in LAHA one needs to add $\cos 4\theta$ components. Once we include these components, the gap along the outer hole FS goes up, bringing the LAHA result even closer to RPA-SF.

We see therefore that the LAHA approximation works quite well both for the bare interaction and the full interaction with the SF contribution. We verified that the near equivalence between gaps obtained within RPA-SF and LAHA holds for all other sets of parameters from Table I. This gives confidence that the physics can be understood by analyzing 4×4 s-wave and d-wave gap equations within LAHA. We begin with the s-wave case.

A. s-wave case

1. *Modification of* $\Gamma_{ij}(\mathbf{k}_F,\mathbf{k}'_F)$ *by spin fluctuations*

We first take a closer look at Table II. Comparing the values of $u_{h_1h_1}, u_{h_2h_2}, u_{h_1h_2}, u_{h_1e}, u_{h_2e}$, and u_{ee} we see two trends. First, once the SF contribution is added, there is overall enhancement, roughly by a factor of three, for *all* interactions, including interactions within hole pockets. On top of this overall enhancement, there is another effect—electron-hole interactions u_{he} further increase compared to u_{hh} and u_{ee}. This additional increase is by a factor of 3–4, such that the total increase of u_{h_1e} is by a factor of 10 (the increase of u_{h_2e} is a bit smaller).

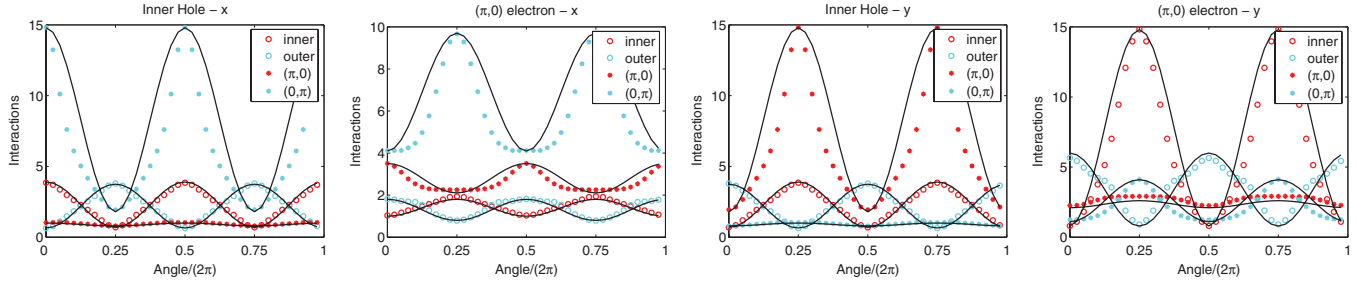

FIG. 2. (Color online) The same as in Fig. 1 but for the full interaction, with SF component. The fit is again reasonably good. We verified that the slight discrepancies are removed if in LAHA we add a 4θ harmonics to the interaction.

TABLE II. s- and d-wave parameters for set 1 with $\mu = 0.08$. Here and henceforth NSF and SF mean the bare interaction without SF component and the full interaction with SF component, respectively.

s wave	$u_{h_1h_1}$	$u_{h_2h_2}$	$u_{h_1h_2}$	u_{h_1e}	α_{h_1e}	u_{h_2e}	α_{h_2e}	u_{ee}	α_{ee}	β_{ee}
NSF	0.8	0.76	0.78	0.46	−0.24	0.4	−0.30	0.77	0.14	0.09
SF	2.27	2.13	2.22	4.65	−0.34	2.29	−0.22	3.67	0.15	0.04
d wave	$\tilde{u}_{h_1h_1}$	$\tilde{u}_{h_2h_2}$	$\tilde{u}_{h_1h_2}$	$\tilde{u}_{h_1e}$	$\tilde{\alpha}_{h_1e}$	$\tilde{u}_{h_2e}$	$\tilde{\alpha}_{h_2e}$	$\tilde{u}_{ee}$	$\tilde{\alpha}_{ee}$	$\tilde{\beta}_{ee}$
NSF	0.7	0.66	−0.68	−0.25	−0.58	0.24	−0.42	0.11	−0.5	0.25
SF	1.50	1.40	−1.50	−3.73	−0.44	1.44	−0.32	1.03	−0.49	−0.02

We attribute the overall increase to the "bare" SF interaction term $u^2\chi_0(q)$ and the additional increase to the relative enhancement of the RPA susceptibility $\chi(Q)/\chi_0(Q)$ near the momentum transfer $Q = (\pi,0)$ or $(0,\pi)$. The reasoning is based on the comparison with the results of Ref. 2 for the bare and RPA-renormalized spin susceptibility. First, the product $u_{ij}\chi_0(\mathbf{k}_i - \mathbf{k}_j)$ remains roughly constant in k space if we use u_{ij} from Table II. Second, the RPA-renormalized $\chi(Q)$ is 3–4 times larger than $\chi_0(Q)$, while $\chi(0) \approx \chi_0(0)$ (Ref. 2). This logic also applies to the interaction between electron pockets, for which u_{ee} is the average between intrapocket interaction, for which $\chi = \chi(0) \approx \chi_0(0)$, and interpocket interaction, for which $\chi = \chi(\pi,\pi) \approx 2.4\chi_0(\pi,\pi)$. The total increase of u_{ee} is then expected to be $1 + 2[(1 + 2.4)/2] = 4.4$, and we see from Table II that u_{ee} increases by a quite similar factor of 4.

Compare next the angular parts α_{he}, α_{ee}, and β_{ee}. We see from Table II that α_{he} and α_{ee} do not change much. The term β_{ee} does change and becomes 2.5 times smaller in the presence of the SF component. However, we will show in the next section that the gap structure is insensitive to the change of β_{ee} and does not change much even if we set $\beta_{ee} = 0$ (see Fig. 5).

Neglecting the change of β_{ee}, we conclude that the SF contribution to the pairing interaction increases the overall magnitude of Γ_{ij} and additionally increases the magnitudes of electron-hole interactions (u_{h_1e} and u_{h_2e} terms) and, to lesser extent, of electron-electron interaction (the u_{ee} term), but does not substantially modify the relevant angular dependence of the electron-hole interaction. The overall increase of the pairing interaction does not affect the gap structure; hence the only true effect of the SF term is the increase of electron-hole interactions compared to hole-hole and electron-electron interactions.

As we said, controlled RG flow of the couplings gives rise to exactly the same effect—angular dependence is preserved during the flow, but the relative magnitude of electron-hole interaction increases. From this perspective, RG and SF approaches, although formally different, describe very similar physics.

2. *Effect of the angular dependencies of electron-hole and electron-electron interactions*

We now analyze explicitly how sensitive the gap structure is to various angular-dependent components of Γ_{ij}. Within LAHA, we can easily change the angular dependence of the interactions and check the consequences. First, we verify how sensitive the solution for the gap is to the change of the angular component of electron-hole interaction.

In Figs. 4 and 5 we show the results for the $s^{\pm}$ gap for different values of α_{h_ie}. Comparing these figures with Fig. 3, we see that the effect of α_{h_ie} on the gap is different for bare and full interaction. For the bare interaction, originally there is no s-wave solution with positive λ_s, but it appears once we increase α_{h_ie} above a certain threshold. This can be easily understood by analyzing the 4×4 gap equation: For bare interaction intrapocket repulsions $u_{h_ih_j}$ and u_{ee} are stronger than interpocket u_{h_ie}; hence the pairing can only be induced by angle-dependent components of the interaction, when the factor S, given by Eq. (17), becomes positive. For original parameters $S < 0$, but once we increase α_{h_ie}, S eventually changes sign and the solution with $\lambda_s > 0$ appears. The gap function for this induced solution has strong oscillations along electron FSs and has accidental nodes.

Consider next the full interaction with the SF component. u_{h_ie} are now enhanced, and the solution with $\lambda_s > 0$ exists even if we set $\alpha_{h_ie} = 0$ (see Fig. 5). The only difference between the solutions with small and larger α_{h_ie} is that in the first case the $s^{\pm}$ gap has no nodes on the two electron FSs. We see therefore that for full interaction the role of α_{h_ie} is merely to modify the already existing $s^{\pm}$ solution and add angular variation to the gap along the two electron FSs.

TABLE III. Strengths of various harmonics of the interactions $\Gamma_{i,j}$ in the s and d channels. We fixed the position on one FS (labeled first) and varied the angle along the other FS. The angle $\psi = \theta$ if on electron FS and ϕ if on hole FS. We used parameter set 2 and $\mu = -0.05$.

	s wave $(h_2 - h_1)$	d wave $(h_2 - h_1)$	s wave $(h_2 - e_1)$	d wave $(h_2 - e_1)$
const.	0.88	0	0.95	0.56
2ψ	0	0.51	0.26	0.26
4ψ	0.01	0	0.13	0.14
6ψ	0	0.05	0.06	0.06
8ψ	0.00	0	0.03	0.03

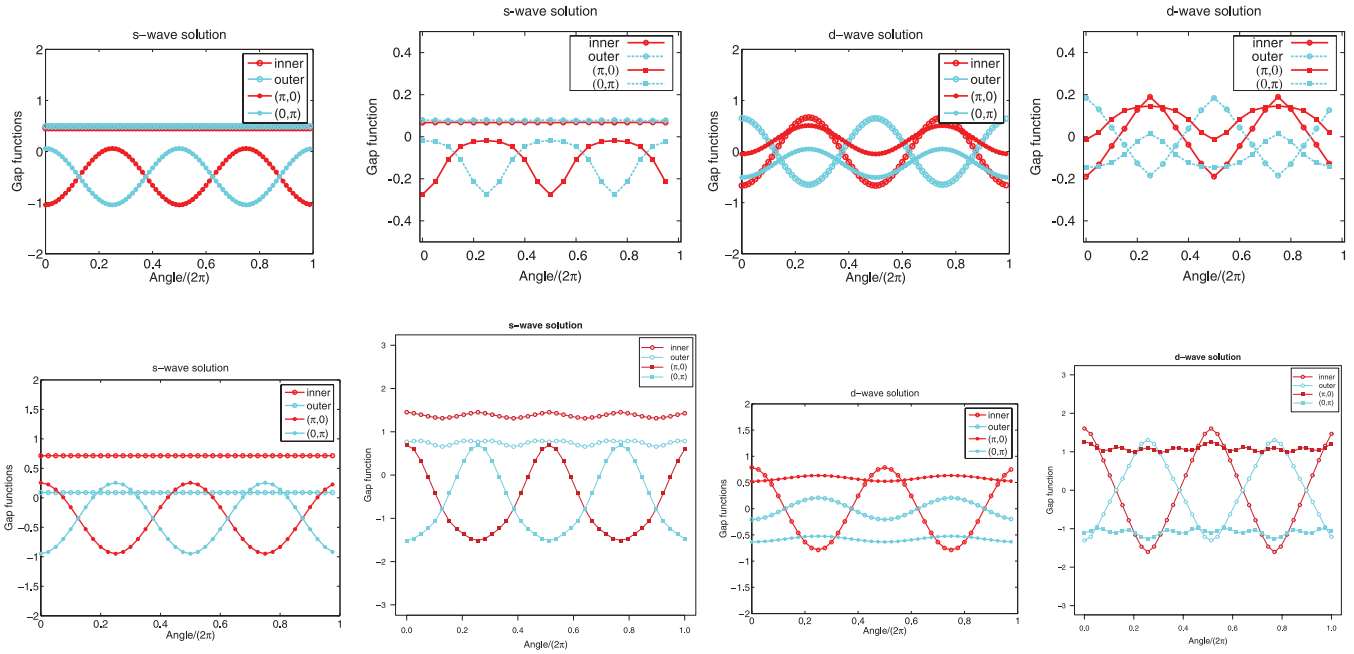

FIG. 3. (Color online) Top: s-wave solutions (left pair) and d-wave solutions (right pair) obtained by applying LAHA for the gap structure for set 1 (NSF) with $\mu = 0.08$ and the ones obtained numerically from the 5-orbital model based on the LDA band structure, respectively. There are no solutions with positive λ, so we show the solutions with the smallest negative λ in both channels. The agreement of the gap structure with LAHA results is quite good. For LAHA, the s-wave solution has $\lambda_s = -1.02$ and the d-wave solution has $\lambda_d = -0.99$ ($\lambda_s/\lambda_d \approx 1.0$). λ_s and λ_d obtained from the numerical approach are negative, and their ratio is $\lambda_s/\lambda_d = 0.6$. Bottom: The same, but now with the SF component of interaction included. The couplings are now positive: $\lambda_s = 4.6$ and $\lambda_d = 4.8$ ($\lambda_s/\lambda_d \approx 0.96$) for LAHA and $\approx$1.1 for RPA-SF calculations for the 5-orbital model (Ref. 1).

We next analyze how sensitive the solution for the gap is to the change of the angular component of electron-electron interaction (α_{ee} and β_{ee} terms). In Fig. 5, bottom panel, we show the results for the gaps obtained with α_{ee} and β_{ee} increased by 2, reduced by 2, and set to zero. Comparing this figure with Fig. 3 (bottom panel) we see that the changes in α_{ee} and β_{ee} lead to very few changes in the gap structure (and the λ's). The gap remains very much the same as in Fig. 3, even if we set α_{ee} and β_{ee} to zero. The implication is that, for full interaction, the gap structure is determined by the angular dependence of electron-hole interaction, while electron-electron interactions can be we approximated by the angle-independent u_{ee} term.

3. *Nodal vs non-nodal s-wave gap for four FSs*

Previous studies of the gap structure for four FSs within RPA-SF formalism yielded the gap with accidental nodes along the electron FS.[1,2] The $s^{\pm}$ solution without nodes only appears for an electronic structure which contains an additional, fifth hole FS centered at (π,π). The results of the previous subsection imply that this result is the likely outcome but is nonuniversal: For the full interaction the

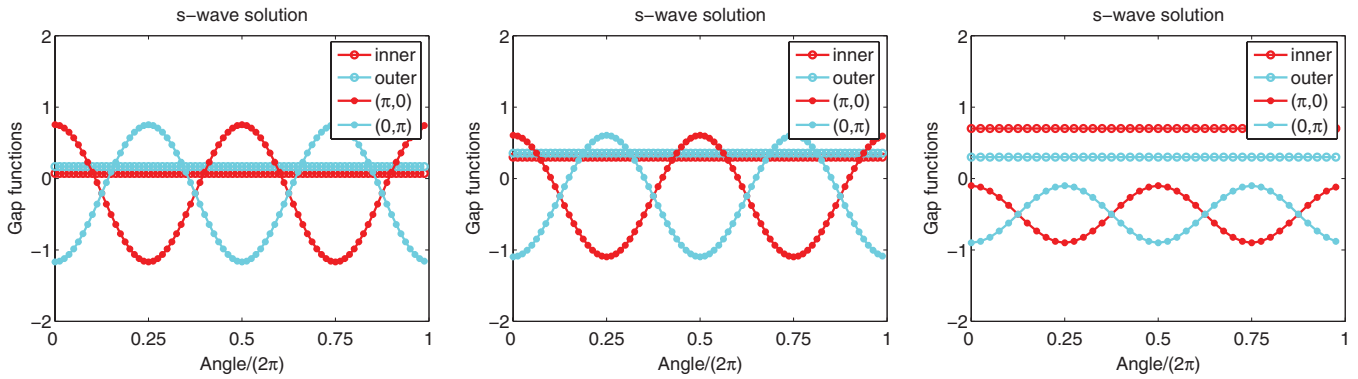

FIG. 4. (Color online) Effect of electron-hole interactions: s-wave solutions for set 1 (NSF) for $\mu = 0.08$ with the angular parts of electron-hole interactions (α_{h_ie}) set to zero and increased by a factor of 2, respectively (left and center). The values of λ_s are -0.16 and 0.226; positive λ_s is for enhanced α_{h_ie}. In the right figure, we introduce additional enhancement of the overall factors of the electron-hole interactions by $\sim$4 and this causes nodes in the gap to disappear.

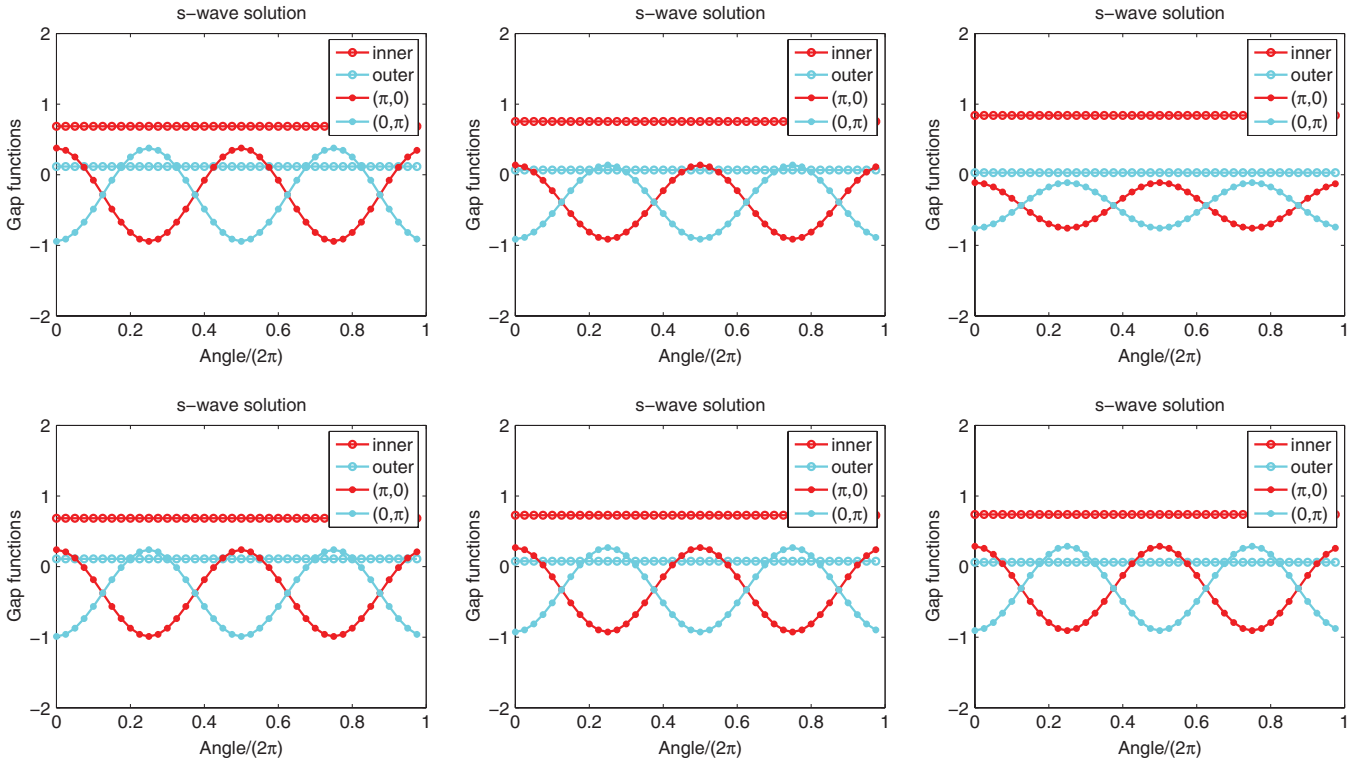

FIG. 5. (Color online) The dependence of the gap structure for s-wave solution on the strength of angle-dependent parts of the interactions. We used set 1 (SF) for $\mu = 0.08$. The solution for the original α_{h_ie} is shown in Fig. 3. Top panel: The gap structure for the cases when the angular parts of the electron-hole interaction (α_{h_ie}) are increased by factor of 2, reduced by factor of 2, and set to zero, while the angular parts of the electron-electron interaction (α_{ee} and β_{ee}) are kept at the original values. The values of λ_s are 7.3, 3.4, and 2.5, respectively. The angular dependence does change, and, in particular, the nodes along the hole FS disappear when we set $\alpha_{h_ie} = 0$. Bottom panel: The same but now we keep α_{h_ie} at the original value and change the angular parts of the electron-electron interactions (α_{ee} and β_{ee} terms): increase them by 2, reduce by 2, and set to zero. The λ's are 4.5, 4.7, and 4.0, respectively. We see that this has very little effect on the structure of the gap.

gap can be either nodeless or with nodes depending on the magnitude of α_{he} and on the interplay between u_{he}^2 and $u_{ee}u_{hh}$ (for simplicity, we set two hole FSs to be equal). When $u_{he}^2 < (u_{ee}u_{hh})$, the only possibility is $s^{\pm}$ pairing with nodes along electron FSs; in the opposite case the solution can be either nodal or nodeless depending on α_{he}. The larger $u_{he}^2/(u_{ee}u_{hh})$ is, the larger α_{he} one needs to make the SC nodal.

To further illustrate this, in Fig. 4 (right) we show the solution of the 4×4 set for the gap for the case when we increase u_{h_1e} and u_{h_2e} keeping all other parameters, including α_{h_ie}, fixed. We see that the nodes on electron FSs disappear for substantially large u_{h_1e} and u_{h_2e}.

In RPA-SF analysis, a way to further increase u_{h_1e} compared to other parameters is to bring the system even closer to AFM instability. For the parameter set we are dealing with, one needs to increase u_{h_ie} by quite substantial amount, so a fine tuning to AFM instability is required to eliminate the nodes. But still, the no-nodal solution definitely exists in some range of parameters.

B. d-wave case

The consideration for the d-wave case proceeds similarly to the s-wave case. The d-wave pairing again can be due to attraction coming from angle-independent parts of the interaction, or it can be induced by angle-dependent parts of the interactions, even when $\lambda_d < 0$ in the absence of angle-dependent terms. We refrain from discussing all cases as in many respects the analysis for d-wave pairing parallels the one for the s-wave case. We point out, however, that the negative λ_d for the case of bare interaction (NSF) is much smaller in magnitude than the coupling in the s-wave channel; i.e., there is "less repulsion" in the d-wave channel. As a result, it takes less to convert the d-wave repulsion into attraction. This can be achieved by shifting the values $\tilde{\alpha}_{h_ie}$, $\tilde{\alpha}_{re}$, and $\tilde{\beta}_{ee}$. Once the SF piece is added to the interaction all d-wave components increase, but, just as for the s-wave case, the largest increase is for electron-hole interaction. This increase is large enough such that the gap equation develops a solution with $\lambda_d > 0$ even if we set angular components of electron-hole and electron-electron interactions to zero. In the latter case, the gaps along the two electron FSs are $\pm\Delta_e$. When we do not set angle-dependent components to zero, electron gaps acquire $\cos 2\theta$ components, but, as we see in Fig. 3, this component is quite small.

We also note that the values of λ_s and λ_d for the full interaction are quite close. For set 1 which we are discussing in this section, we found that, within LAHA, λ_d is actually a bit larger than λ_s, for the parameters extracted from the fit, but λ_d and λ_s are very close and λ_s becomes larger already after a small change of parameters. The solution for the gap within RPA also shows that, for this set, λ_s and λ_d are very close,

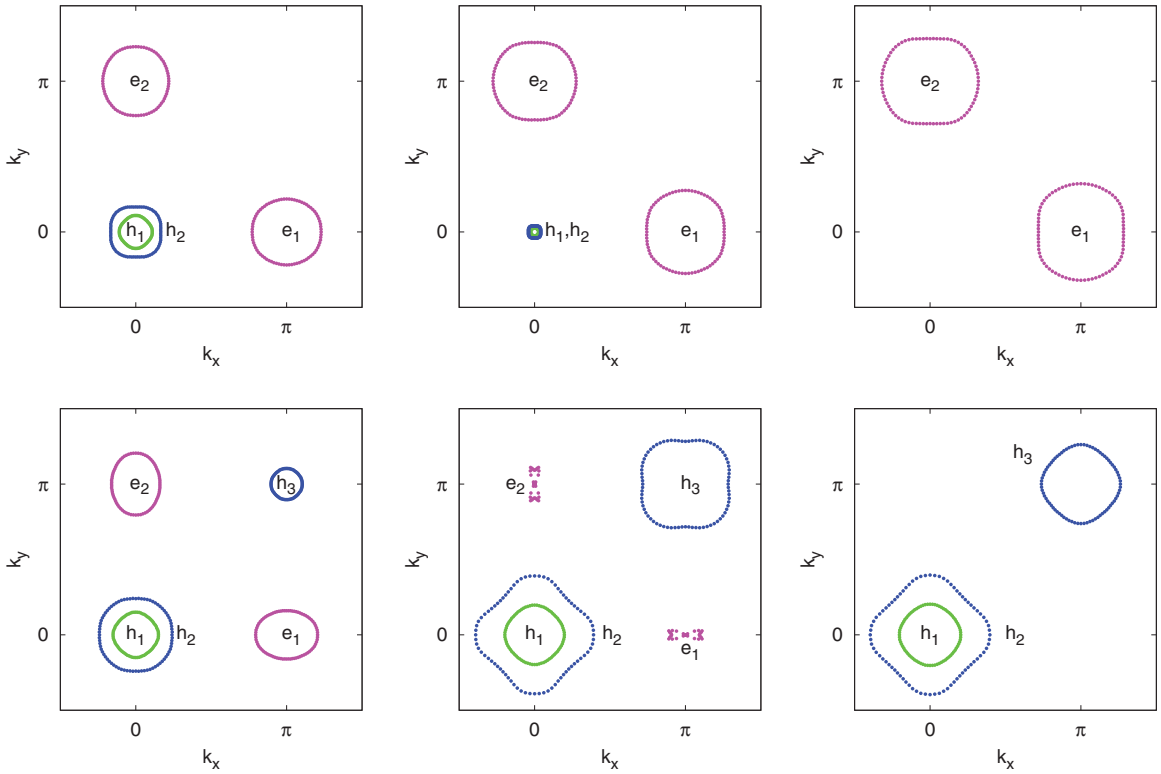

FIG. 6. (Color online) Top, left to right: FSs for increasing electron doping with $\mu = 0.05, 0.18, 0.30$, respectively. $\mu = 0.18$ represents the electron doping at which the hole FS almost disappears, while $\mu = 0.30$ represents extreme electron doping where the hole FS completely disappears. Bottom, left to right: FSs for increasing hole doping with $\mu = -0.05, -0.18, -0.20$, respectively. Here electron FSs almost disappear at $\mu = -0.18$ and completely disappear at $\mu = -0.20$.

but it yields $\lambda_s \geqslant \lambda_d$. In any event, however, s-wave coupling λ_s definitely becomes stronger than λ_d once the system comes close enough to an antiferromagnetic instability.

IV. DOPING EVOLUTION OF s-WAVE AND d-WAVE GAP FUNCTIONS

To understand the evolution with doping, we choose set 2 for definiteness and consider the gap structure for positive and negative values of the chemical potential. Positive μ corresponds to electron doping and negative μ corresponds to hole doping. For positive μ, the electronic structure consists of two hole and two electron pockets, and the size of the hole pockets becomes smaller as μ increases. For negative μ, the electronic structure contains an additional, fifth hole pocket, centered at (π,π). As before we shall denote the electron pocket at $(\pi,0)$ as e_1, the electron pocket at $(0,\pi)$ as e_2, the inner hole pocket at $(0,0)$ as h_1, the outer hole pocket at $(0,0)$ as h_2, and the hole pocket at (π,π) when present as h_3. In this section we only consider moderate doping, when both hole and electron FSs are present. We consider the limiting case of large electron and hole dopings in the next section. For simplicity, we only present results for full interaction with the SF component.

A. Electron doping

We considered several values of electron doping (positive μ). Below we present the results for the representative case of $\mu = 0.05$ ($n_e = 6.09$). The FS is presented in Fig. 6. In Table IV we present LAHA s-wave and d-wave interaction components from Eq. (10), obtained by fitting RPA-SF results. The actual fits are presented in Fig. 7, where we present the best and the worst fits. We see that even the worst fits are actually quite reasonable. In the same figure we show s-wave and d-wave gaps corresponding to the largest λ_s and λ_d.

The tables show the same trends that we discussed in the previous section; the most relevant one is the overall increase of all interactions when the SF component is added, and further increase of electron-hole interaction in both s-wave and d-wave channels. In this section we focus on the features associated with the dependence on doping. For briefness, we show only the case of full interaction with the SF component.

First, we see from Fig. 7 that for positive μ (when the electronic structure consists of four FSs), the s-wave solution with $\lambda_s > 0$ has nodes on the electron FSs. The d-wave solution with $\lambda_d > 0$ has symmetry-related nodes on the hole FSs, but no nodes on electron FSs. That $\lambda_d > 0$ is the combination of the two effects: (i) The d-wave component of the interaction between electron pockets is negative ($\tilde{u}_{ee} < 0$); i.e., there is a direct d-wave attraction between electron pockets. (ii) The d-wave components of electron-hole interaction $\tilde{u}_{h_1e}$ and $\tilde{u}_{h_2e}$ are quite large. Both effects give rise to $\lambda_d > 0$ even if we set all $\cos 2\theta$ components of the interactions to zero. Within LAHA, we can check the relative importance of the two effects by artificially setting one of them to zero. We see from Tables IV and V that $\tilde{u}_{ee}$ is attractive, but very weak. The primary reason for $\lambda_d > 0$ are large values of electron-hole interaction $\tilde{u}_{h_1e}$

TABLE IV. s- and d-wave parameters for set 2 with $\mu = 0.05$.

s wave	$u_{h_1h_1}$	$u_{h_2h_2}$	$u_{h_1h_2}$	u_{h_1e}	α_{h_1e}	u_{h_2e}	α_{h_2e}	u_{ee}	α_{ee}	β_{ee}
NSF	0.51	0.50	0.50	0.32	−0.19	0.28	−0.24	0.50	0.11	0.08
SF	0.80	0.79	0.79	0.79	−0.19	0.67	−0.19	0.91	0.05	0.05
d wave	$\tilde{u}_{h_1h_1}$	$\tilde{u}_{h_2h_2}$	$\tilde{u}_{h_1h_2}$	$\tilde{u}_{h_1e}$	$\tilde{\alpha}_{h_1e}$	$\tilde{u}_{h_2e}$	$\tilde{\alpha}_{h_2e}$	$\tilde{u}_{ee}$	$\tilde{\alpha}_{ee}$	$\tilde{\beta}_{ee}$
NSF	0.38	0.36	−0.37	−0.14	−0.60	0.14	−0.60	0.05	−0.6	0.35
SF	0.50	0.49	−0.50	−0.39	−0.46	0.30	−0.47	−0.04	1.5	−0.69

and $\tilde{u}_{h_2e}$. Accordingly, the driving force for d-wave attraction is the strong d-wave component of the pair-hopping between electron and hole pockets. In this respect, the mechanism is quite similar to that for the sign-changing s-wave gap.

How far in electron doping does this mechanism remain the leading one? To analyze this, we also considered the case of a larger $\mu = 0.18$ ($n_e = 6.23$), when hole pockets almost disappear. The FS for this case is shown in Fig. 6, the parameters extracted from the fit are shown in Table V, and the fits and the gaps are presented in Fig. 8. A somewhat surprising result is that there is very little change compared to the case of smaller $\mu = 0.05$, when hole pockets are much larger. Still, the dominant interaction in the d-wave channel is the pair hopping between hole and electron FSs. The d-wave component of electron-electron interaction is negative (i.e., attractive), but it remains very small.

Note also that for both μ's $\lambda_d > \lambda_s$, and the difference increases as electron doping increases. This does not necessarily mean that the d-wave is the leading instability because T_c for s-wave and d-wave superconducting instabilities have different prefactors. Still, a larger value of λ_d implies that d-wave superconductivity is certainly a possibility in electron-doped pnictides. A more exotic mixed $s + id$ state is also quite possible,[40] but to study it one obviously needs to solve a nonlinear gap equation, which is beyond the scope of this work.

B. Hole doping

We next consider representative cases of hole doping by setting μ to negative values, $\mu = -0.05$ ($n_e = 5.95$) and $\mu = -0.18$ ($n_e = 5.53$). In Fig. 6 we show the FS for these two μ's. The FS now has an additional hole pocket centered at (π,π). For $\mu = -0.05$ hole and electron pockets are of comparable size; for $\mu = -0.18$, the electron pockets almost disappear. The fits to LAHA for $\mu = -0.05$ are presented in Fig. 9 and the parameters extracted from the fits are summarized in Table VI. We see from Fig. 9 that for hole doping the situation is different in two aspects. First, the s-wave gap has no nodes; second, λ_s is substantially larger than λ_d; i.e., s-wave superconductivity is the most likely scenario. To understand these differences, compare Table IV with Table VI. We see that the interactions between two hole FSs at (0,0) and two electron FSs do not change substantially between electron-doped and hole-doped cases, but for the hole-doped case there appear additional hole-hole and hole-electron interactions associated with the fifth hole pocket. These additional interactions are weak and irrelevant for the d-wave component of $\Gamma_{ij}(\mathbf{k}_F,\mathbf{k}'_F)$, but are quite strong for the s-wave component. We analyzed the 5×5 gap equation for the s-wave gap, and found that these additional interactions effectively increase the angle-independent component of the electron-hole interaction, which favors the no-nodal $s^{\pm}$ gap. As a consequence, the system develops an $s^{\pm}$ solution with relatively large $\lambda_s > 0$, even if all interactions are set to be angle independent. When we include the angle-dependent components, the gap acquires some momentum dependence along electron FSs, but for given parameters this dependence is weak and the gap remains nodeless. There is no "theorem," however, that the $s^{\pm}$ solution is always nodeless for five FS pockets. In Fig. 11 we show the gap for the full interaction for the set 3. We see that the gap does in fact have nodes on the electron FSs.

We also note that, for the d-wave case, the electron-electron interaction $\tilde{u}_{ee}$ is repulsive, and the d-wave solution with $\lambda_d > 0$ is again the result of relatively strong d-wave electron-hole interactions $\tilde{u}_{h_1e}$ and $\tilde{u}_{h_2e}$ involving the two hole pockets centered at (0,0).

The outcome of the study so far is quite simple: The no-nodal $s^{\pm}$ solution is the leading instability if the angle-independent part of the electron-hole interaction u_{he} (either the direct one or the effective one, in case of five FSs) is sufficiently large compared to $(u_{hh}u_{ee})^{1/2}$. In the opposite case, the s-wave solution has nodes on electron FSs, and $d_{x^2-y^2}$ pairing is a strong competitor.

Consider next how far in doping the nodeless $s^{\pm}$ gap remains the leading instability. To analyze this, we turn to the case of $\mu = -0.18$, when the electron pockets almost disappear. The FS for this case is shown in Fig. 6, the

TABLE V. s- and d-wave parameters for set 2 with $\mu = 0.18$.

s wave	$u_{h_1h_1}$	$u_{h_2h_2}$	$u_{h_1h_2}$	u_{h_1e}	α_{h_1e}	u_{h_2e}	α_{h_2e}	u_{ee}	α_{ee}	β_{ee}
NSF	0.56	0.55	0.56	0.30	−.23	0.29	−0.23	0.52	0.12	0.06
SF	0.75	0.75	0.74	0.67	−0.19	0.67	−0.20	0.88	0.10	0.05
d wave	$\tilde{u}_{h_1h_1}$	$\tilde{u}_{h_2h_2}$	$\tilde{u}_{h_1h_2}$	$\tilde{u}_{h_1e}$	$\tilde{\alpha}_{h_1e}$	$\tilde{u}_{h_2e}$	$\tilde{\alpha}_{h_2e}$	$\tilde{u}_{ee}$	$\tilde{\alpha}_{ee}$	$\tilde{\beta}_{ee}$
NSF	0.43	0.43	−0.43	−0.14	−0.62	0.14	−0.62	0.04	−0.625	0.44
SF	0.51	0.51	−0.51	−0.32	−0.50	0.32	−0.50	−0.05	0.9	−0.6

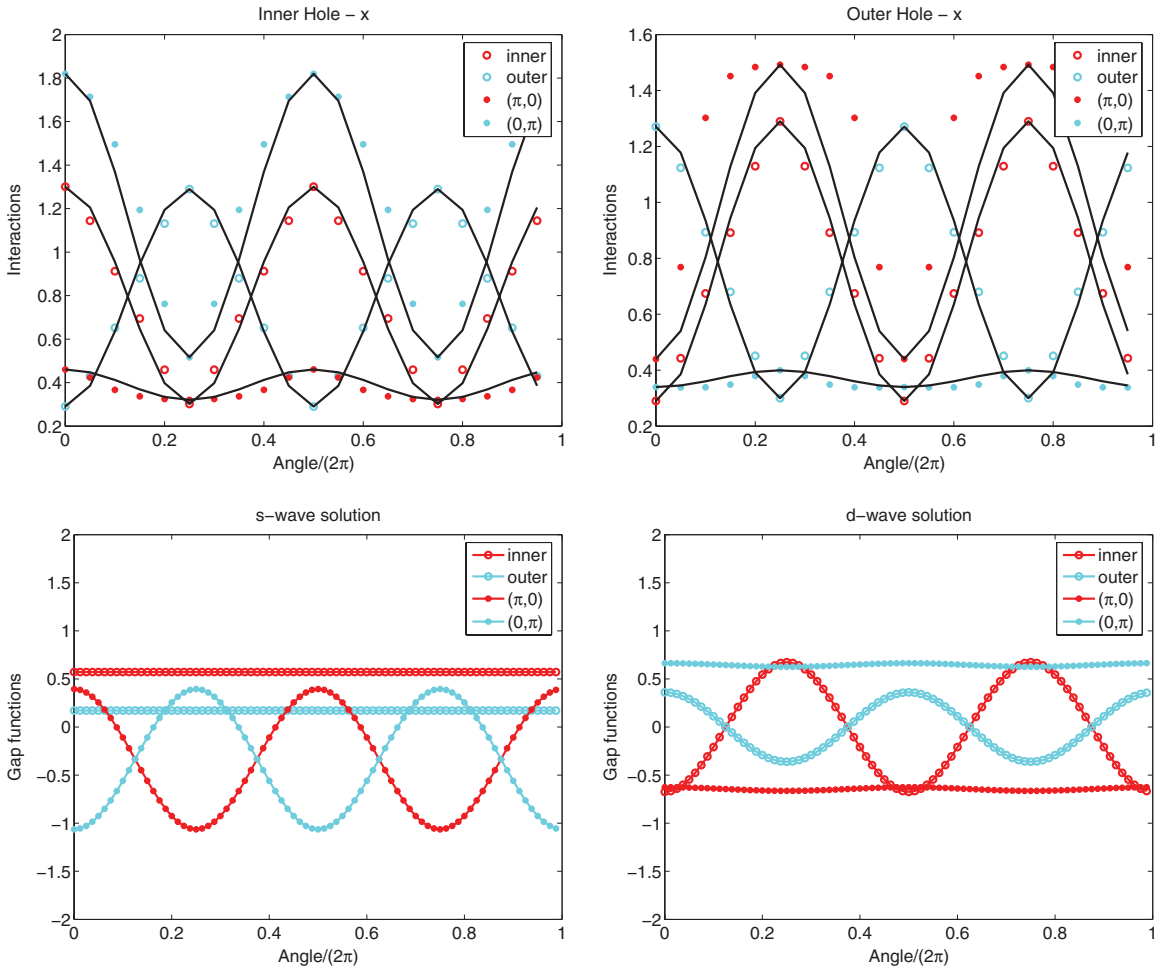

FIG. 7. (Color online) Top panel: The best and worst LAHA fits of the interactions $\Gamma(\mathbf{k}_F,\mathbf{k}'_F)$ obtained from RPA-SF calculations for parameter set 2 (SF) for $\mu = 0.05$. Bottom panel: Gap functions in s and d channels obtained in the LAHA. $\lambda_s = 0.25$, $\lambda_d = 0.37$. Note that λ_d is somewhat larger.

parameters extracted from the fit are shown in Table VII, and the fits and the gaps are presented in Fig. 10.

On analyzing the structure of the interactions and the gaps and comparing them to the case of $\mu = -0.05$ we see that the key features survive despite the small size of the electron pockets. Namely, the leading instability remains $s^{\pm}$, the gap has no nodes, and the driving force for the pairing is the interaction between hole and (still existing) electron pockets. The d-wave channel is a competitor ($\lambda_d > 0$), but still, $s^{\pm}$ state has larger λ.

The conclusion of this subsection is that, as long as both hole and electron pockets are present, the pairing instability is essentially driven by electron-hole interaction. This should obviously change at even larger hole or electron dopings, when only one type of pocket remains and the pairing (if it exists) should come from the interaction either between hole pockets or between electron pockets.

V. OVERDOPING

Finally, we consider the case of strong electron or hole doping, when hole FSs disappear and only electron ones at $(0,\pi)$ and $(\pi,0)$ remain, and the case of strong hole doping,

TABLE VI. s- and d-wave parameters for set 2 with $\mu = -0.05$.

s wave	$u_{h_1h_1}$	$u_{h_2h_2}$	$u_{h_3h_3}$	$u_{h_1h_2}$	$u_{h_1h_3}$	$u_{h_2h_3}$	u_{h_1e}	α_{h_1e}	u_{h_2e}	α_{h_2e}	u_{h_3e}	α_{h_3e}	u_{ee}	α_{ee}	β_{ee}
NSF	0.50	0.49	1.00	0.49	0.20	0.13	0.34	−0.18	0.30	−0.25	0.61	0.26	0.49	0.11	0.10
SF	0.86	0.96	1.83	0.89	0.45	0.32	0.92	−0.18	0.79	−0.21	1.5	0.21	1.00	0.11	0.08
d wave	$\tilde{u}_{h_1h_1}$	$\tilde{u}_{h_2h_2}$	$\tilde{u}_{h_3h_3}$	$\tilde{u}_{h_1h_2}$	$\tilde{u}_{h_1h_3}$	$\tilde{u}_{h_2h_3}$	$\tilde{u}_{h_1e}$	$\tilde{\alpha}_{h_1e}$	$\tilde{u}_{h_2e}$	$\tilde{\alpha}_{h_2e}$	$\tilde{u}_{h_3e}$	$\tilde{\alpha}_{h_3e}$	$\tilde{u}_{ee}$	$\tilde{\alpha}_{ee}$	$\tilde{\beta}_{ee}$
NSF	0.36	0.36	0	−0.36	0	−0	−0.15	−0.58	0.15	−0.58	−0	−0.58	0.06	−0.58	0.33
SF	0.51	0.61	0.01	−0.56	0.00	−0.01	−0.45	−0.48	0.39	−0.43	0.02	0.90	0.07	−1.00	0.46

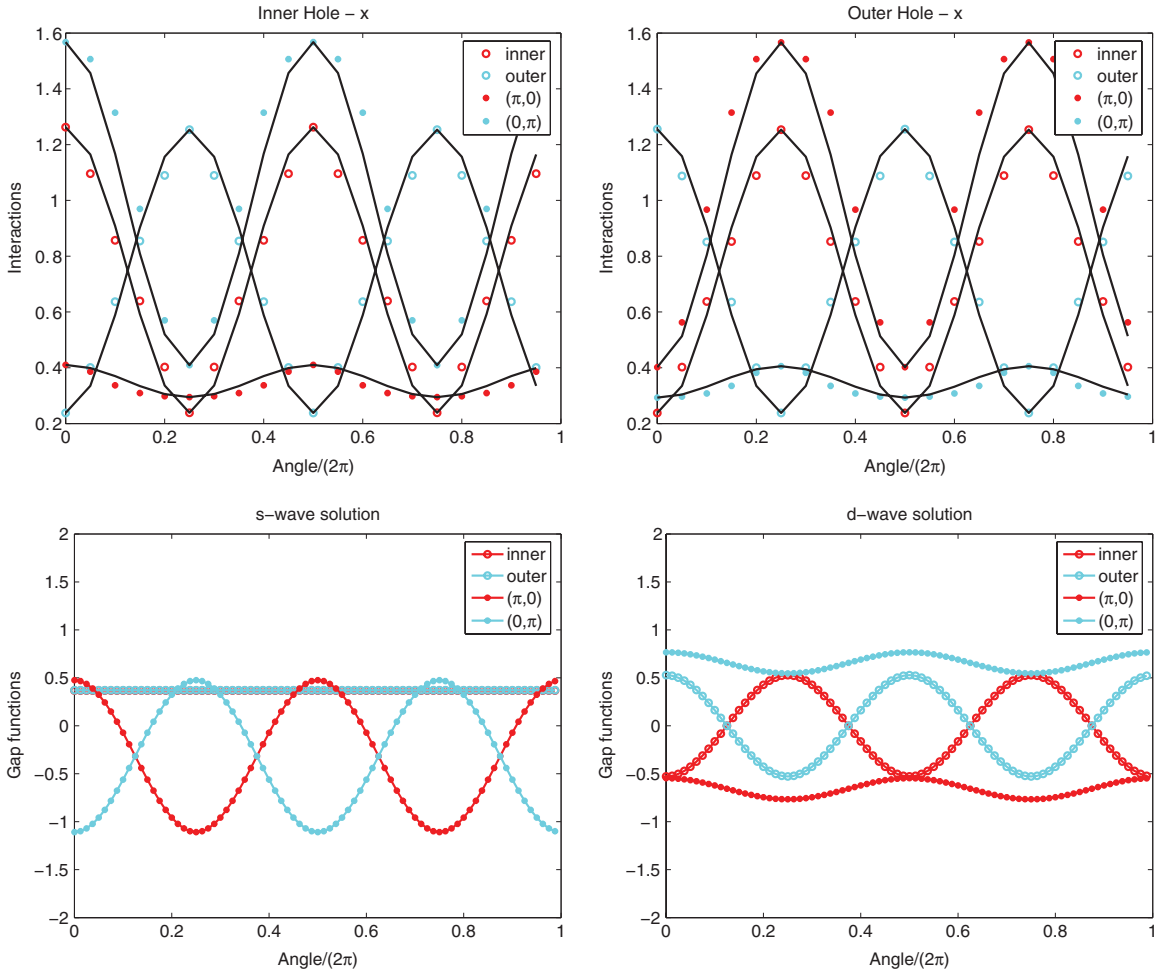

FIG. 8. (Color online) The same as in Fig. 7, but for different $\mu = 0.18$. $\lambda_s = 0.21$, $\lambda_d = 0.35$. Again, λ_d is larger, and the difference between λ_d and λ_s is larger than for $\mu = 0.05$.

when electron FSs disappear and only hole FSs at (0,0) and (π,π) remain. We consider the two limits separately.

A. Strong electron doping

Strongly electron-doped FeSCs include recently discovered FeSe superconductors AFe_2Se_2 (A = K, Rb, Cs).[32] T_c in these materials is quite high and reaches almost 40 K. The electronic structure of these materials in the folded Brillouin zone is a bit more involved because (i) AFe_2Se_2 has body-centered tetragonal structure that makes the folding of the electron FSs a more complex procedure than just the mixing of the two ellipses which would be the case for a simple tetragonal structure,[14,36] and (ii) there is apparently a small electron pocket at (0,0).[33] Because our main intention is to understand what causes the pairing in the absence of hole pockets, we follow Ref. 26 and neglect the peculiarities of the folding procedure and potential electron pocket at (0,0). Corrections to this approach have been discussed in Refs. 36 and 14.

RPA-SF and fRG studies[26,30,31] applied to AFe_2Se_2 showed that the dominant instability is in the d-wave channel. The issue we want to address is whether the interaction between the two electron pockets alone is capable of giving rise to sizable d-wave attraction for large positive μ. We recall in this regard that for the two cases of electron doping that we considered before ($\mu = 0.05$ and $\mu = 0.18$), the direct electron-electron interaction was attractive but very small, and the attraction in the d-wave channel was primarily the result of the strong d-wave component of electron-hole interaction. Recall that at $\mu = 0.18$ the hole FSs are already very small. Hole excitations are visible in ARPES in AFe_2Se_2 above the gap of 60–100 meV (Refs. 33), and it is certainly a possibility that the dominant mechanism of d-wave attraction between fermions on electron FSs in AFe_2Se_2 is virtual pair hopping to gapped hole states.

Let us elaborate on this point. When hole FSs are present, this pair hopping give rise to an effective attractive d-wave interaction between electron pockets with magnitude $\tilde{u}_{he}^2 L$, where $L = \log E_F/T_c$ comes from integration over low-energy hole states. This interaction can well exceed a direct $\tilde{u}_{ee}$ because for relevant values of the logarithm $\tilde{u}_{he}L = O(1)$. (A way to see this is to express Δ_h via Δ_e in the matrix gap equation and rewrite it solely as an equation for Δ_e.) When hole excitations are gapped, the logarithm is cut and scales as $L = \log[E_F/(T_c^2 + E_0^2)]$, where E_0 is the gap for hole states. Because in AFe_2Se_2 $E_0 \leqslant E_F$ (Ref. 33) it is not *a priori* guaranteed that $\tilde{u}_{eh}L$ is now small and can be neglected. The fRG study of superconductivity in AFe_2Se_2 (Ref. 30) does include this contribution because

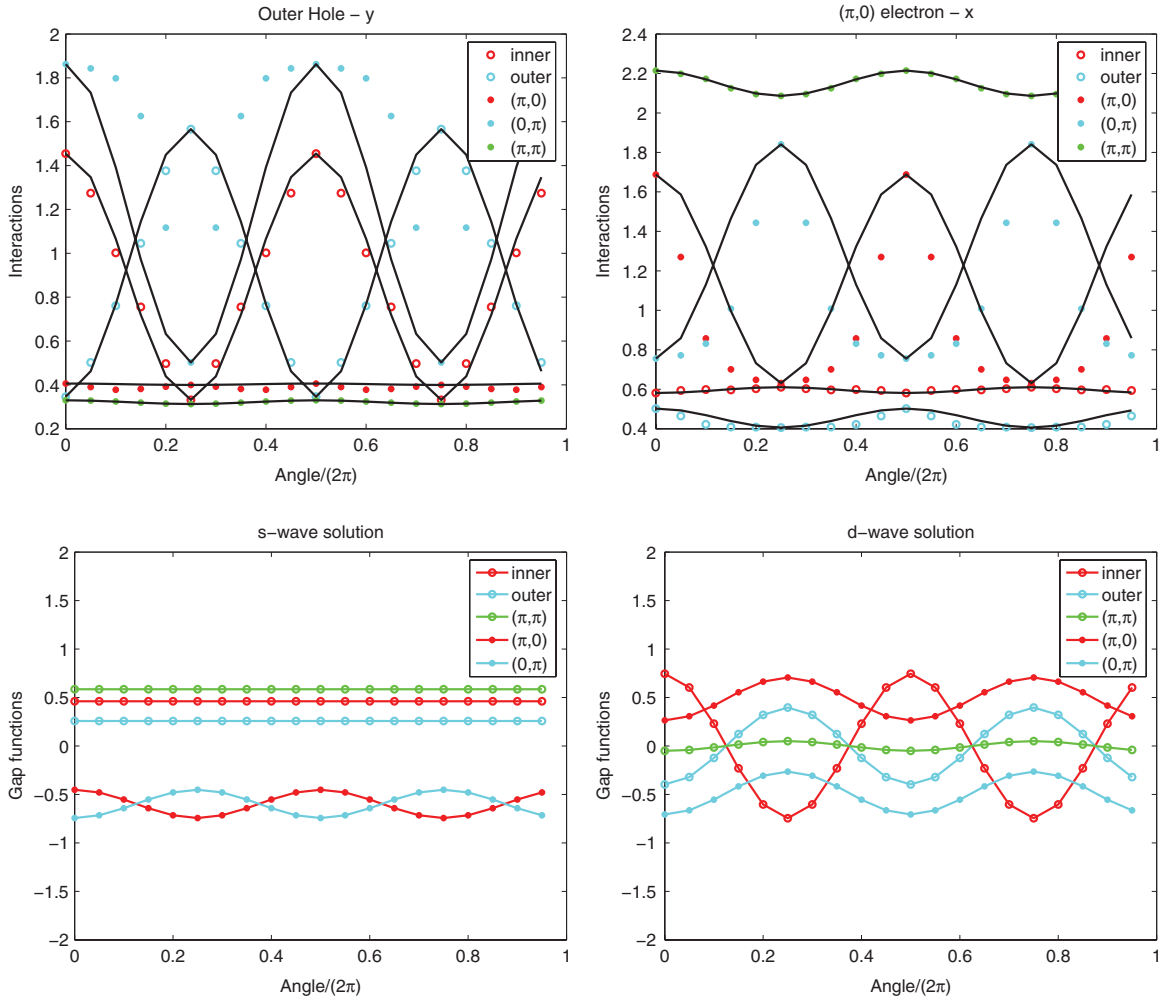

FIG. 9. (Color online) The same as in Fig. 7, but for negative $\mu = -0.05$, when extra hole FS appears. $\lambda_s = 0.58$, $\lambda_d = 0.31$. Observe that now $\lambda_s > \lambda_d$ and the $s^{\pm}$ gap has no nodes.

the RG procedure incorporates renormalizations coming from energies above E_F.

A way to verify whether the direct electron-electron interaction or the pair hopping to gapped hole states is the dominant mechanism of d-wave attraction in AFe_2Se_2 is to use the RPA-SF approach which only considers the interaction between fermions right at the FSs and neglects pairing interactions via intermediate gapped states, and see whether λ_d is large enough (e.g., comparable to λ_s for hole doping), and whether the d-wave gap structure is similar to that obtained in fRG which includes virtual processes via gapped states. If λ_d is not small and the gap structure is similar to that in fRG, electron-hole interaction is likely irrelevant, and d-wave attraction comes from the direct electron-electron interaction.

In Fig. 12 we show the fit to electron-electron interactions obtained in RPA-SF formalism to Eq. (10) in which we only kept electron-electron interactions. The parameters in the s-wave and d-wave channels extracted from the fit are shown in Table VIII. We solved 3×3 gap equations in s-wave and d-wave channels with these parameters and show the results in Fig. 12. We clearly see that d-wave eigenvalue is positive.

For completeness, we also computed the d-wave eigenvalue for a different band structure, used in Ref. 26, which still has only electron FSs remaining. The results are shown in Fig. 12

TABLE VII. s- and d-wave parameters for $\mu = -0.18$. For technical reasons we used $U = 0.9$, $J = 0$, and $V = 0.9$.

s wave	$u_{h_1h_1}$	$u_{h_2h_2}$	$u_{h_3h_3}$	$u_{h_1h_2}$	$u_{h_1h_3}$	$u_{h_2h_3}$	u_{h_1e}	α_{h_1e}	u_{h_2e}	α_{h_2e}	u_{h_3e}	α_{h_3e}	u_{ee}	α_{ee}	β_{ee}
NSF	0.37	0.37	0.74	0.36	0.04	0.10	0.40	0.0	0.40	0.0	0.04	0.0	0.44	0.0	0.0
SF	0.75	2.02	17.2	0.98	−0.08	0.41	1.36	0.08	2.86	0.02	0.31	−0.01	1.40	0.01	0.06
d wave	$\tilde{u}_{h_1h_1}$	$\tilde{u}_{h_2h_2}$	$\tilde{u}_{h_3h_3}$	$\tilde{u}_{h_1h_2}$	$\tilde{u}_{h_1h_3}$	$\tilde{u}_{h_2h_3}$	$\tilde{u}_{h_1e}$	$\tilde{\alpha}_{h_1e}$	$\tilde{u}_{h_2e}$	$\tilde{\alpha}_{h_2e}$	$\tilde{u}_{h_3e}$	$\tilde{\alpha}_{h_3e}$	$\tilde{u}_{ee}$	$\tilde{\alpha}_{ee}$	$\tilde{\beta}_{ee}$
NSF	0.36	0.36	0	−0.36	−0.04	0.04	−0.40	−0.0	0.40	−0.0	0.04	−0.0	0.44	−0.0	0.0
SF	0.70	1.94	13.6	−0.94	0.04	0.33	−1.32	0.0	2.85	0.02	0.26	0.02	1.45	0.01	0.04

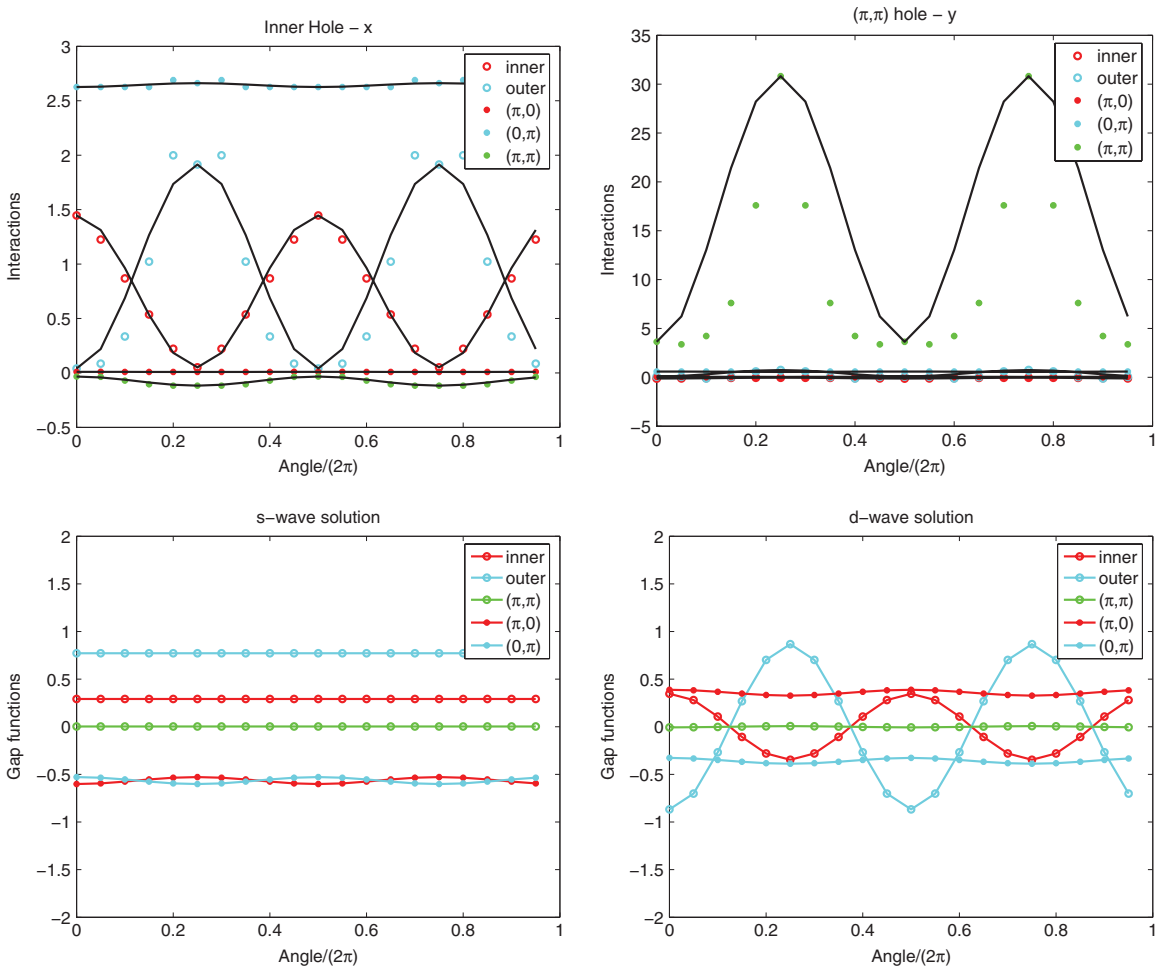

FIG. 10. (Color online) The same as in Fig. 9, but for $\mu = -0.18$ and $U = 0.9, J = 0.0, V = 0.9$. We obtain $\lambda_s = 1.8$, $\lambda_d = 1.2$. Observe that, still, $\lambda_s > \lambda_d$ and the $s^{\pm}$ gap has no nodes.

and Table IX. We find that the d-wave eigenvalue is again positive and the d-wave gap structure is quite similar to that in Fig. 12. The magnitude of λ_d, however, depends on the choice of the band structure.

With the LAHA fit, we are in a position to analyze the pairing in more detail and check whether the d-wave attraction comes from angle-independent or angle-dependent parts of the electron-electron interaction. In the absence of hole FSs, λ_d is the solution of the 2×2 gap equation and is given by

$$\lambda_d = -\tilde{u}_{ee}\left(2\tilde{\beta}_{ee} + 1 \pm \left[(2\tilde{\beta}_{ee} - 1)^2 + 8\tilde{\alpha}_{ee}^2\right]^{1/2}\right). \quad (18)$$

In general, $\lambda_d > 0$ either because $\tilde{u}_{ee} < 0$, or $\tilde{u}_{ee} > 0$ but $\tilde{\alpha}_{ee}^2 > \tilde{\beta}_{ee}$. In the first case, the d-wave gap is due to a direct attraction between fermions from the two electron pockets, much in analogy with the "hot spot" scenario for the cuprates, and the gap has only modest variation along the electron FSs and no nodes. In the second case, the d-wave gap should have nodes. We see from Tables VIII and IX that $\tilde{u}_{ee} < 0$; i.e., d-wave attraction in AFe_2Se_2 is primarily due to the existence of a constant (angle-independent) attractive d-wave interaction between the two electron pockets.

To understand why $\tilde{u}_{ee} < 0$ we remind the reader that $\tilde{u}_{ee}$ is the difference between intrapocket and interpocket electron-electron interactions $\tilde{u}_{ee} = (N_F/2)(\Gamma_{e_1e_1} - \Gamma_{e_1e_2})$ [see Eq. (10)]. The bare values of $\Gamma_{e_1e_1}$ and $\Gamma_{e_1e_2}$ are quite close. For small electron doping, magnetic fluctuations are predominantly peaked at $(0,\pi)$ and $(\pi,0)$, and neither of these two interactions are selected for relative increase. As a result, the full intrapocket and interpocket electron-electron interactions remain of nearly equal magnitude, and the difference between the two is small. Once the hole pockets disappear, the peak in magnetic susceptibility shifts to near (π,π), according to RPA.[26] In this situation, SF enhances the interpocket $\Gamma_{e_1e_2}$ compared to the intrapocket $\Gamma_{e_1e_1}$, and $\tilde{u}_{ee}$ becomes negative (attractive).

We also note that the s-wave solution remains attractive for one choice of the band structure (see Table IX), although

TABLE VIII. s- and d-wave parameters for the case of strong electron doping, when there are no hole FSs.

s wave	u_{ee}	α_{ee}	β_{ee}	λ_s
	0.84	0.09	0.04	−0.12
d wave	$\tilde{u}_{ee}$	$\tilde{\alpha}_{ee}$	$\tilde{\beta}_{ee}$	λ_d
	−0.04	0.88	−0.75	0.13

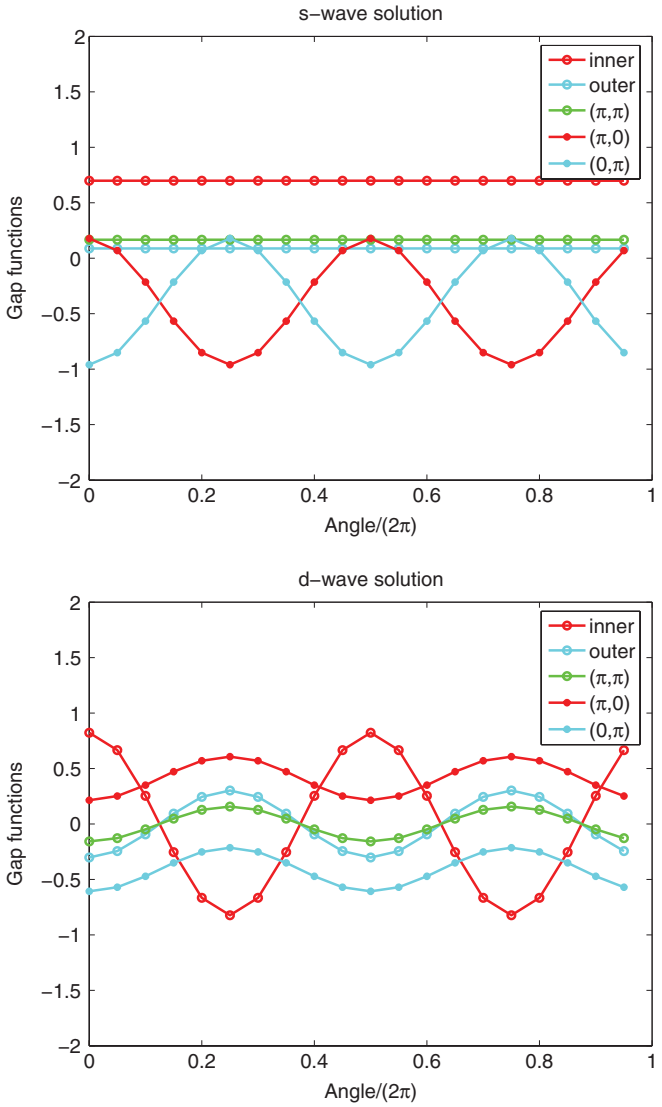

FIG. 11. (Color online) $s^{\pm}$ gap structure obtained within LAHA for parameter set 3 (SF) for $\mu = -0.05$. The coupling $\lambda_s = 0.79$. The gap has nodes on electron FS despite that there is the third Fermi surface at (π,π). This nodal solution has a strong d-wave competitor for which $\lambda_d = 0.8$.

$\lambda_s < \lambda_d$. The two solutions for λ_s are given by

$$\lambda_s = -u_{ee}\left(2\beta_{ee} + 1 \pm \left[(2\beta_{ee} - 1)^2 + 8\alpha_{ee}^2\right]^{1/2}\right). \quad (19)$$

The interaction u_{ee} is given by $u_{ee} = (N_F/2)(\Gamma_{e_1e_1} + \Gamma_{e_1e_2})$ and is positive when both intrapocket $\Gamma_{e_1e_1}$ and interpocket $\Gamma_{e_1e_2}$ are positive, as in Tables IX and VIII. For $u_{ee} > 0$ a positive λ_s appears when $\alpha_{ee}^2 > \beta_{ee}$ which is satisfied for the parameters in Table IX. Such a solution is induced by angle-dependent electron-electron interaction terms, and the s-wave gap should have nodes on the electron FSs. This is consistent with Fig. 12.

The structure of both d-wave and s-wave gap functions is also quite consistent with the solution obtained within fRG.[30] The authors of that paper argued that the attraction in the d-wave channel is due to virtual hopping to gapped hole states, which is captured in fRG. We, on the contrary, believe that the good agreement between fRG and the LAHA-RPA approach, which does not include gapped hole states, indicates that the primary cause for a d-wave pairing is the direct interaction between the two electron pockets, present in both approaches. We have not investigated the influence of gapped hole states directly, however.

The issue that we do not discuss in this paper is how the d-wave gap evolves under the transformation into the folded zone. The folding is a nontrivial procedure for the case of d-wave pairing because the two electron FSs do hybridize in the folded zone, and this frustrates the d-wave gap which changes sign between the two unhybridized FSs. Further complication is that AFe_2As_2 has a body-centered tetragonal lattice, and the two electron FSs which eventually hybridize differ by $k_z = \pi$ and are rotated by $\pi/2$ before hybridization. There is an argument that in this situation the d-wave gap must have nodes near $k_z = \pi/2$ (see Ref. 36). However, the issue of the pairing in the presence of the hybridization is not settled at the moment and we will not dwell on it.

Finally, in our discussion we assumed that both intrapocket interaction $\Gamma_{e_1e_1}$ and interpocket interaction $\Gamma_{e_1e_2}$ are positive. Then u_{ee} is definitely positive. Intrapocket interaction is certainly positive, but the sign of interpocket interaction depends on the interplay between U, V, J, and J' in the same way as the sign of u_{he} depends on the interplay between intraorbital and interorbital interactions. If $\Gamma_{e_1e_2} < 0$ the d-wave $\tilde{u}_{ee} = (N_F/2)(\Gamma_{e_1e_1} + |\Gamma_{e_1e_2}|)$ becomes positive, while the s-wave $u_{ee} = (N_F/2)(\Gamma_{e_1e_1} - |\Gamma_{e_1e_2}|)$ becomes negative, if $|\Gamma_{e_1e_2}| > \Gamma_{e_1e_1}$. In this situation, the system develops an s-wave pairing with equal sign of the gap on the two hole pockets. We make a conjecture that $\Gamma_{e_1e_2}$ is negative if one uses the orbital J_1-J_2 model with the interaction between first and second neighbors in real space (and $J_2 > J_1$), instead of the on-site orbital Hubbard-Hund model. This would explain why both strong-coupling[34,35] and weak-coupling[35] studies of the pairing in the orbital J_1-J_2 model yielded an s-wave pairing.

B. Strong hole doping

Superconductivity at strong hole doping, when only hole FSs are present, has been observed in KFe_2As_2,[41,42] which is at the opposite end from parent $BaFe_2As_2$ in the family of $K_{1-x}Ba_xFe_2As_2$. T_c in this material is rather low, only 3 K, but the interest in KFe_2As_2 is fueled by the fact that penetration depth and thermal conductivity measurements point to nodal behavior, much as in LaFePO. The fRG study by Thomale *et al.*[29] shows that the leading instability is in the d-wave channel, consistent with the observation of nodes. Interestingly, Thomale *et al.* have found that the d-wave gaps on the three hole FSs [two centered at (0,0) and one at (π,π)] are "in phase" with each other, i.e., $\Delta_i(\phi) = \Delta_i \cos 2\phi$ ($i = 1$–3), and all Δ_i are of the same sign. This is *not* the d-wave solution with the largest λ_d at smaller doping, when both hole and electron pockets are present. In that solution, there is a π phase shift between the gaps on the two FSs centered at (0,0) (see Figs. 10 and 9). The solution with "in phase" d-wave gaps is one of five d-wave solutions in the LAHA formalism, but with negative λ_d at small to moderate hole doping.

Given this discrepancy, it is interesting to analyze strong hole doping in our approach. For this, we set $\mu = -0.20$

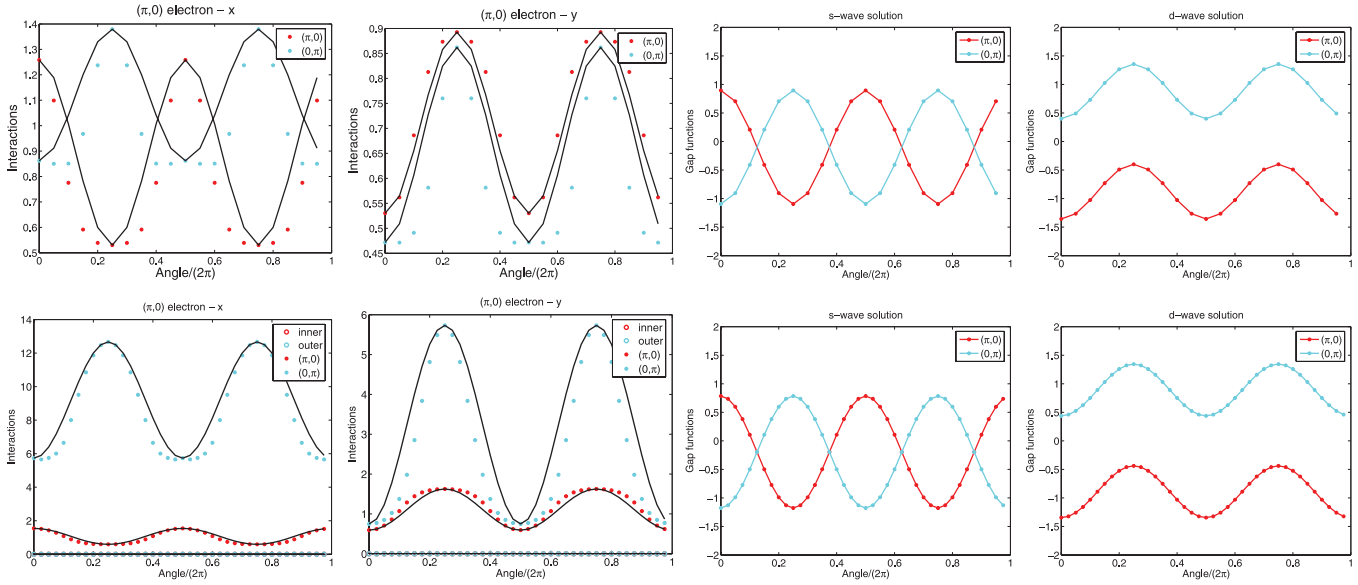

FIG. 12. (Color online) Top: The fits of the interactions and the structure of s-wave and d-wave gaps in LAHA for the case of heavy electron doping, when only electron FSs are present. The λ's are $\lambda_s = -0.12$ and $\lambda_d = 0.13$ ($\mu = 0.30$). Bottom: The same, but for a different band structure, used in Ref. 26. The couplings are $\lambda_s = 0.1$ and $\lambda_d = 5.9$.

and consider $U = 1$, $J = 0.25$, $V = 0.6$, which is a rescaled version of the interactions used by Thomale *et al.* This is done to avoid a magnetic instability in the RPA-SF analysis. For the parameters from Ref. 2, we changed ϵ_{3z2-r2} from -0.211 to -0.511 to leave only one of two (π,π) hole pockets, see Fig. 6.

The results for the fit of the RPA-SF interactions to LAHA and s-wave and d-wave gap structures are shown in Fig. 13, and the interaction parameters extracted from the fit are presented in Table X. We see that the d-wave solution is attractive, while for the s-wave solution the largest λ_s is negative. We verified, however, that it can be also made positive either by a slight change of $u_{h_i h_j}$ or by the inclusion of $\cos 4\phi$ terms, so in essence s-wave and d-wave λ's are comparable. What does not depend on small variation of parameters is that both s-wave and d-wave solutions are different from the corresponding solutions at smaller $|\mu|$, when hole and electron FSs were present. In particular, we see from Fig. 13 that the s-wave gap now changes sign between the two hole FSs centered at (0,0), while in the d-wave solution the gaps on these two FSs are "in phase." We remind the reader that at smaller $|\mu|$ the s-wave gaps on the two hole FSs are of the same sign, while the d-wave gaps on these FSs have a phase shift of π (see Figs. 10 and 9).

TABLE IX. s- and d-wave parameters for the case of strong electron doping, with band structure from Ref. 26, when there are no hole FSs.

s-wave	u_{ee}	α_{ee}	β_{ee}	λ_s
	3.65	0.20	0.03	0.1
d-wave	$\tilde{u}_{ee}$	$\tilde{\alpha}_{ee}$	$\tilde{\beta}_{ee}$	λ_d
	-2.57	0.29	-0.0	5.9

Also, for the d-wave case, a straightforward analysis of the 3×3 d-wave gap equation shows that the solution with $\lambda_d > 0$ exists for two reasons, both specific to the absence of electron pockets. First, we see from Table X that the d-wave intrapocket interaction within the (π,π) pocket, $\tilde{u}_{h_3,h_3}$, is now negative (i.e., attractive). Second, intrapocket interaction $\tilde{u}_{h_1,h_2}$ between the two pockets at (0,0) is negative and larger in magnitude than repulsive $\tilde{u}_{h_1,h_1}$ and $\tilde{u}_{h_2,h_2}$. In consequence, if we momentarily decouple the pocket at (π,π) and the two pockets at (0,0), we obtain two solutions with positive λ_d. One corresponds to a gap only on the (π,π) pocket, another to in-phase gaps on the two pockets at (0,0). The third solution is the one in which there is the π phase shift between the two gaps at (0,0). This solution has negative λ_d and is irrelevant. The residual, much weaker interaction between the pockets at (0,0) and (π,π) couples the two solutions with positive λ_d and sets the phase shift between the gaps at (π,π) and (0,0). In each of these two coupled solutions, there is no phase shift between the gaps at (0,0), and the gap at (π,π) is larger than the gaps at (0,0) simply because $\tilde{u}_{h_3,h_3}$ is attractive while $\tilde{u}_{h_1,h_1}$ and $\tilde{u}_{h_2,h_2}$ are repulsive. These features are not present in the d-wave solution with the largest λ_d for smaller $|\mu|$, when both hole and electron FSs are present. For those cases, $\tilde{u}_{h_3,h_3}$ is repulsive, and there is a π phase shift between the two gaps at (0,0) because $\tilde{u}_{h_1,h_2}$ is dominated by the interactions with electron pockets $\tilde{u}_{h_1 e}$ and $\tilde{u}_{h_2 e}$ which, by symmetry, are of different signs. We see therefore that the two d-wave solutions of the linearized gap equation which give the two largest λ_d are not the same as the solution with the largest λ_d at smaller $|\mu|$.

The larger value of Δ_{h_3} compared to Δ_{h_1} and Δ_{h_2} and the in-phase structure of the gaps at (0,0) are consistent with the fRG d-wave solution by Thomale *et al.*[29] There is only one relatively minor disagreement: For our parameters the solution with the largest λ_d is the one for which the (π,π) gap and (0,0) gaps have relative phase shift π, i.e., are "of opposite sign"

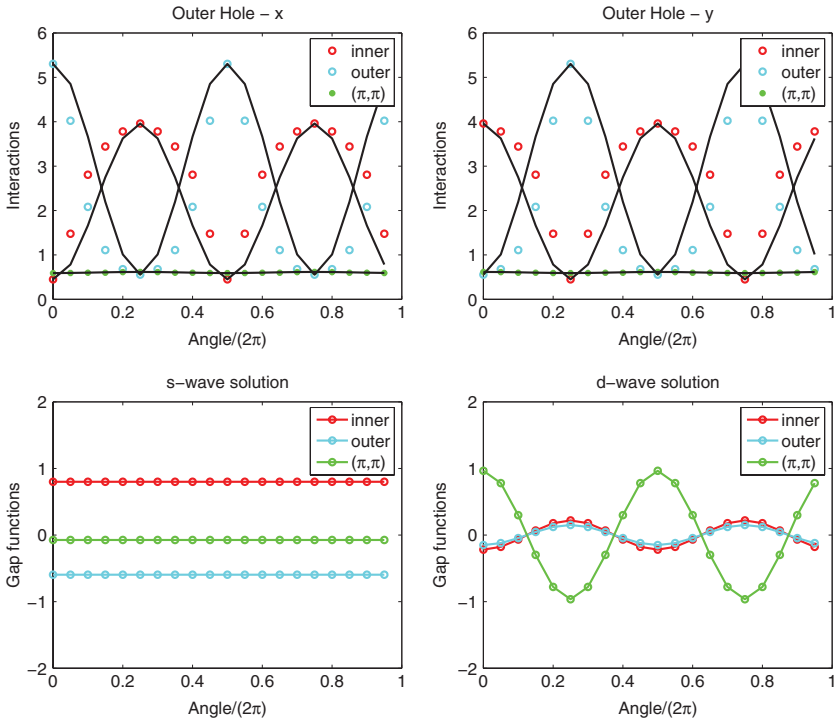

FIG. 13. (Color online) The fits of the interactions by LAHA and the structure of s-wave and d-wave gaps for the case of heavy hole doping, $\mu = -0.20$, when only hole FSs are present. The parameters are $U = 1, J = 0.25, V = 0.69$ (see text). The eigenvalues are $\lambda_s = -.05$ and $\lambda_d = 0.05$.

(see Table XI). Thomale *et al.* found the solution with the "equal sign" of all three d-wave gaps. We verified, however, that the selection of the phase between (π,π) and $(0,0)$ gaps is sensitive to the interplay between $\tilde{u}_{h_1,h_3}$ and $\tilde{u}_{h_2,h_3}$, which are small in magnitude and have different signs (see Table X). Already a small modification of these parameters makes λ_d larger for the solution with the same phase for the gaps on all three FSs, the same as in the fRG solution.

The pairing in heavily hole doped FeSCs was recently studied within RPA for the five-band orbital model by Suzuki *et al.*[27] They found that s-wave and d-wave pairing amplitudes are of about the same strength. This agrees with our analysis. There is one difference, however: Suzuki *et al.* argued that the pairing interaction predominantly comes from the interaction between hole states and gapped electron states near $(0,\pi)$ and $(\pi,0)$, while in our case the pairing comes from the interaction between hole pockets. Suzuki *et al.* cited recent observations of incommensurate spin fluctuations in KFe_2As_2 (Ref. 43) as evidence for still strong interactions between fermions from near Γ and (π,π) points and from near $(0,\pi)$ and $(\pi,0)$. This is certainly a possibility, but we point out that the interaction within the hole pocket centered at (π,π) also gives rise to incommensurate spin fluctuations at rather large momenta, because of a large size of that pocket. We recall that in our theory, the magnetically enhanced interaction within the (π,π) hole pocket is the driving force for the d-wave pairing.

TABLE X. s- and d-wave parameters for the case of strong hole doping (with SF component), when there are no electron FSs.

s wave	$u_{h_1h_1}$	$u_{h_2h_2}$	$u_{h_3h_3}$	$u_{h_1h_2}$	$u_{h_1h_3}$	$u_{h_2h_3}$	λ_s
	1.75	2.93	1.97	2.20	0.63	0.60	−0.05
d wave	$\tilde{u}_{h_1h_1}$	$\tilde{u}_{h_2h_2}$	$\tilde{u}_{h_3h_3}$	$\tilde{u}_{h_1h_2}$	$\tilde{u}_{h_1h_3}$	$\tilde{u}_{h_2h_3}$	λ_d
	1.34	2.37	−0.09	−1.76	−0.01	0.05	0.05

C. Strong electron vs strong hole doping

We see that in our theory there is an attraction in the d-wave channel at both strong hole doping and strong electron doping (at least, for the model and parameters which we considered). The two limits are, however, quite different from a physics perspective. For the case of strong electron doping, the enhancement of the spin susceptibility around (π,π) unambiguously leads to an attraction in the d-wave channel, i.e., to $\lambda_d > 0$. For strong hole doping, the susceptibility is peaked at $(0,0)$, which affects $\tilde{u}_{h_1,h_1}$, $\tilde{u}_{h_1,h_2}$, $\tilde{u}_{h_2,h_2}$, and $\tilde{u}_{h_3,h_3}$. The attractive d-wave solution is the result of negative $\tilde{u}_{h_3,h_3}$ and a larger value of $\tilde{u}^2_{h_1,h_3}$ compared to $\tilde{u}_{h_1,h_1}\tilde{u}_{h_2,h_2}$. There is no fundamental reason why it should be so except that for large noncircular Fermi surfaces in 2D, the particle-hole susceptibility $\chi(q)$ is larger at $2k_F$ than at $q = 0$ and the appearance of the solution with a positive λ_d at strong hole doping is very likely accidental. In other words, similar materials without electron pockets could be s-wave or d-wave superconductors.

VI. CONCLUSIONS

In this paper we analyzed the pairing symmetry and the structure of the gap in FeSCs by approximating the pairing interaction between low-energy fermions by leading

TABLE XI. The structure of d-wave gaps $\Delta_{h_i}(\phi_i) = \Delta_{h_i}\cos 2\phi_i$ for $\mu = -0.20$ obtained by solving 3×3 linearized gap equation (the gaps are in arbitrary units since only the ratios of the gaps matter).

	Solution 1	Solution 2	Solution 3
Δ_{h_1}	0.22	0.77	0.60
Δ_{h_2}	0.15	0.58	−0.80
Δ_{h_3}	−0.96	0.27	0.01
λ	**0.05**	−0.02	−1.84

angular harmonics. This allowed us to decompose the pairing interaction and study separately contributions to pairing from scattering processes between different FSs and the interplay between angle-independent and angle-dependent parts of each interaction. The angular dependence of the interactions is peculiar to FeSCs because of the multiorbital nature of low-energy excitations. (The interactions in band representation are obtained by dressing up interactions in orbital representation by angle-dependent coherence factors associated with the hybridization of Fe-d orbitals.) We used the band interaction obtained within RPA-SF formalism as an input, fitted it within LAHA, verified that the fit is quite good for all cases that we studied, and analyzed in detail how the pairing interactions in s-wave and d-wave channels evolve with the bare interaction and the one with the extra SF component and between hole and electron doping. We also analyzed the interplay between s-wave and d-wave pairing. Using the same procedure, we also studied the pairing at large electron (hole) doping, when only electron (hole) FSs are present. Throughout this paper we treated FeSCs as quasi-2D systems and did not address potential new physics associated with 3D effects.

The main conclusion of our study is that all pairing states obtained so far at different dopings in FeSCs can be understood within the same universal pairing scenario based on spin-fluctuation exchange. We furthermore found that all these pairing states appear naturally in the effective low-energy model with a small number of input parameters. We conjecture that the approaches based on RPA (both analytical and functional) and on the itinerant J_1-J_2 model reduce to this model at low energies, however with different input parameters.

We used this effective model to study the doping evolution of the pairing in hole- and electron-doped FeSCs. We argue that the pairing mechanisms at small-to-moderate and large dopings are qualitatively different—when both hole and electron pockets are present, the pairing is of Kohn-Luttinger type, driven by the pair hopping of fermions from hole to electron pockets, while at larger hole or electron doping, the pairing is due to a direct interaction between only hole or only electron pockets. For moderate hole dopings the leading pairing instability is toward an $s^{\pm}$ state with a nodeless gap. For moderate electron doping a nodal $s^{\pm}$ state is the leading instability, but the d wave is a close competitor. For larger electron or hole dopings, when only one type of FS is present, the leading pairing instability is toward a d-wave state, which in the case of strong electron doping is nodeless, at least in the 2D case.

We summarize below the detailed reasoning behind the observation stated above by presenting the answers to the questions we posed in the introduction.

(1) *What is the origin of the strong angular dependence of the $s^{\pm}$ gap along the electron FSs?*

We found that the origin is different for bare and full interactions. For bare interactions (no SF component), the combination of intra- and inter-electron-pocket repulsions are stronger than the electron-hole interaction and the $s^{\pm}$ attractive solution for the gap is entirely due to the angle-dependent parts of the electron-hole (electron-electron for strongly electron-doped materials) interaction, much as was anticipated in Refs. 1 and 44. Namely, the system adjusts the magnitude of the angle-dependent, $\pm\cos 2\theta$ gap component along the two electron FSs to minimize the effect of the inter-electron-pocket repulsion.

For the full interaction, the electron-hole interaction is the strongest, and the attractive $s^{\pm}$ solution exists even if all interactions are taken to be angle independent. The angle-dependent terms modify the $s^{\pm}$ gap by creating $\pm\cos 2\theta$ gap components. Whether these components are large enough to lead to nodes depends on details, but the generic trend is that when the angle-independent part of the electron-hole interaction is larger, the gap is less likely to have nodes.

(2) *Are the angular dependencies of all interactions relevant for the gap structure, or can some interactions be safely approximated as angle independent?*

We found that the angle-dependent part of the electron-hole interaction is the relevant one. The angle-dependent parts of the electron-electron interaction have little effect on the gap structure, at least for the full interaction with the SF component.

(3) *Why do the $s^{\pm}$ solutions obtained within the RPA-SF and fRG approaches have nodes for systems with two hole and two electron FSs and no nodes for systems with three hole and two electron FSs?*

We found that the angle-independent electron-hole interaction, which favors a no-nodal $s^{\pm}$ gap, is further increased if the third hole FS is present. For most of the parameter sets which we analyzed, the $s^{\pm}$ gap has nodes in case of electron doping (four FSs), but the no-nodal solution is stabilized for hole doping (five FSs). Kuroki *et al.*[3] have pointed out that this can be traced back to the d_{xy} orbital character of the third hole pocket which interacts strongly with the d_{xy} states at the tips of the electron pockets. We found, however, that for some parameters nodal solutions survive in the presence of the fifth FS; i.e., the disappearing of the nodes with the appearance of the fifth FS is not a universal result. That aside, the gap structure still evolves between nodal and no nodal once we change the magnitudes of the angle-dependent parts of the interactions.

(4) *What causes the pairing when only electron FSs are present?*

We found that the d-wave pairing is generally attractive and competes with $s^{\pm}$ pairing for the electron-doped FeSC. At small electron doping, the d-wave attraction is almost entirely due to the d-wave electron-hole interaction, and the direct d-wave interaction between electron pockets is weak. For strong electron doping, when only electron FSs are present, the situation is different. We found an *attractive* d-wave interaction between electron pockets. The d-wave pairing is then quite similar to the one in the magnetic hot-spot pairing scenario for the cuprates. In both cases, there is a d-wave attraction between the FS sheets separated by (π,π).

With regard to the subleading s-wave attraction, in our case it is due to an angle-dependent s-wave component of the electron-electron interaction. We did not consider the interaction via gapped hole states (another potential reason for the s-wave attraction), but the similarity between our gap structure and the one obtained in the fRG study,[30] which includes both interactions, indicates that the likely origin of the s-wave attraction is the angle dependence of the electron-electron interaction.

(5) *What causes the pairing when only hole FSs are present?*

We found that both d-wave and s-wave superconductivity is possible. The d-wave channel is favorable in LAHA, but subleading terms may tilt the balance toward s wave.

The reason for the s-wave instability is a strong repulsive interpocket (h_1-h_2) interaction between the two pockets at (0,0), which exceeds the intrapocket repulsion. This leads to a sign-changing s-wave gap between the two hole pockets, in full analogy with the sign-changing solution in a model with strong interpocket interaction between hole and electron pockets.

The reason for the competing d-wave instability is twofold. First, the d-wave component of the intrapocket interaction within the hole pocket at (π,π) is negative (i.e., attractive); second, there is strong attractive d-wave interaction between the two hole pockets at (0,0). The combination of these two reasons leads to a $d_{x^2-y^2}$ solution with positive λ_d, in which the magnitude of the gap is the largest on the (π,π) pocket, and the two gaps at (0,0) have zero phase shift.

Both s-wave and d-wave solutions are different from the ones at smaller hole dopings, when hole and electron FSs are present [e.g., the d-wave solution with the largest λ_d at smaller $|\mu|$ is the one with the π phase shift between the two gaps at (0,0)].

(6) *How is the structure of the pairing interaction affected when the spin-fluctuation component is added to the direct fermion-fermion interaction?*

We found that the SF interaction primarily changes the overall magnitude of the interaction, while its angular dependence remains nearly unchanged. All components of the pairing interaction increase when the SF term is added. On top of this, there is an additional increase of the hole-electron interpocket interaction, both in the s-wave and in the d-wave channels. This additional increase makes both s-wave and d-wave solutions attractive.

We also found that the competition between s-wave and d-wave channels exists at all doping levels. The only exception is the case of small hole doping, when nodeless s-wave pairing is a clear winner. As either hole or electron doping increases, the ratio λ_d/λ_s increases; i.e., the tendency toward a d-wave superconductivity gets stronger. For strong hole doping, d-wave and s-wave couplings are comparable, but for strong electron doping we find d-wave pairing as a clear winner.

We note, however, that we have only studied the strictly 2D case thus far, and neglected aspects of the 3D $I4/mmm$ crystal symmetry characteristic of 122 materials and the hybridization of electron pockets in the folded zone. The hybridization may play a substantial role, particularly for the d-wave state at strong electron doping. We nevertheless believe that the general evolution of interactions and gap symmetry discussed here will be generic to the FeSCs. The approach developed here can be easily modified to study superconductivity on hybridized FSs and can also be used to study in great detail SDW instability in multiorbital systems.[45]

ACKNOWLEDGMENTS

We acknowledge helpful discussions with L. Benfatto, R. Fernandes, W. Hanke, I. Eremin, H. Kontani, K. Kuroki, Y. Matsuda, I. Mazin, R. Prozorov, D. Scalapino, J. Schmalian, Z. Tesanovic, R. Thomale, M. Vavilov, and A. Vorontsov. This work was supported by NSF-DMR-0906953 (S.M. and A.V.C.). Partial support from MPI PKS (Dresden) (S.M. and A.V.C.) and the Humboldt Foundation (A.V.C.) is gratefully acknowledged. T.A.M. acknowledges support from the Center of Nanophase Materials Sciences, which is sponsored at Oak Ridge National Laboratory by the Office of Basic Energy Sciences, US Department of Energy. M.M.K. and P.J.H. acknowledge support from DOE DE-FG02-05ER46236. M.M.K. is grateful for support from RFBR (Grant No. 09-02-00127), Presidium of RAS program N5.7, FCP Scientific and Research-and-Educational Personnel of Innovative Russia for 2009-2013 (GK P891 and GK 16.740.12.0731), and the President of Russia (Grant No. MK-1683.2010.2).

[1] T. A. Maier, S. Graser, D. J. Scalapino, and P. J. Hirschfeld, Phys. Rev. B **79**, 224510 (2009).
[2] S. Graser, T. A. Maier, P. J. Hirshfeld, and D. J. Scalapino, New J. Phys. **11**, 025016 (2009).
[3] K. Kuroki, H. Usui, S. Onari, R. Arita, and H. Aoki, Phys. Rev. B **79**, 224511 (2009).
[4] H. Ikeda, R. Arita, and J. Kunes, Phys. Rev. B **81**, 054502 (2010).
[5] A. F. Kemper, T. A. Maier, S. Graser, H-P. Cheng, P. J. Hirschfeld, and D. J. Scalapino, New J. Phys. **12**, 073030 (2010).
[6] S. Graser, A. F. Kemper, T. A. Maier, H. P. Cheng, P. J. Hirschfeld, and D. J. Scalapino, Phys. Rev. B **81**, 214503 (2010).
[7] C. Platt, C. Honerkamp, and Werner Hanke, New J. Phys. **11**, 055058 (2009); R. Thomale, C. Platt, J. Hu, C. Honerkamp, and B. A. Bernevig, Phys. Rev. B **80**, 180505 (2009).
[8] R. Thomale, C. Platt, W. Hanke, and B. A. Bernevig, Phys. Rev. Lett. **106**, 187003 (2011).
[9] F. Wang, H. Zhai, and D.-H. Lee, Phys. Rev. B **81**, 184512 (2010).
[10] V. Cvetkovic and Z. Tesanovic, Phys. Rev. B **80**, 024512 (2009).
[11] A. V. Chubukov, Physica C **469**, 640 (2009); A. V. Chubukov, D. V. Efremov, and I. Eremin, Phys. Rev. B **78**, 134512 (2008).
[12] S. Maiti and A. V. Chubukov, Phys. Rev. B **82**, 214515 (2010).
[13] Y. Bang and H-Y. Choi, Phys. Rev. B **78**, 134523 (2008).
[14] H. Kontani and S. Onari, Phys. Rev. Lett. **104**, 157001 (2010).
[15] T. Saito, S. Onari, and H. Kontani, Phys. Rev. B **83**, 140512(R) (2011).
[16] T. Shimojima *et al.* (unpublished).
[17] M. Daghofer, A. Moreo, J. A. Riera, E. Arrigoni, D. J. Scalapino, and E. Dagotto, Phys. Rev. Lett. **101**, 237004 (2008); A. Moreo, M. Daghofer, J. A. Riera, and E. Dagotto, Phys. Rev. B **79**, 134502 (2009).
[18] For recent reviews on the itinerant approach see, e.g., P. J. Hirschfeld, M. M. Korshunov, and I. I. Mazin, Rep. Prog. Phys. **74**, 124508 (2011).
[19] D. J. Singh and M.-H. Du, Phys. Rev. Lett. **100**, 237003 (2008).

[20]C. Weber, K. Haule, and G. Kotliar, Nat. Phys. **6**, 574 (2010).
[21]L. Ortenzi, E. Cappelluti, L. Benfatto, and L. Pietronero, Phys. Rev. Lett. **103**, 046404 (2009).
[22]E. Abrahams and Q. Si, J. Phys. Condens. Matter **23**, 223201 (2011); Q. Si *et al.*, New J. Phys. **11**, 045001 (2009).
[23]M. M. Parish, J. Hu, and B. A. Bernevig, Phys. Rev. B **78**, 144514 (2008).
[24]M. J. Calderon, B. Valenzuela, and E. Bascones, Phys. Rev. B **80**, 094531 (2009).
[25]K. Kuroki, S. Onari, R. Arita, H. Usui, Y. Tanaka, H. Kontani, and H. Aoki, Phys. Rev. Lett. **101**, 087004 (2008).
[26]T. A. Maier, S. Graser, P. J. Hirschfeld, and D. J. Scalapino, Phys. Rev. B **83**, 100515(R) (2011).
[27]K. Suzuki, H. Usui, and K. Kuroki, Phys. Rev. B **84**, 144514 (2011).
[28]T. A. Maier and D. J. Scalapino, e-print arXiv:1107.0401.
[29]R. Thomale, C. Platt, W. Hanke, J. Hu, and B. A. Bernevig, Phys. Rev. Lett. **107**, 117001 (2011).
[30]F. Wang, F. Yang, M. Gao, Z.-Y. Lu, T. Xiang, and D.-H. Lee, Europhys. Lett. **93**, 57003 (2011).
[31]T. Das and A. V. Balatsky, Phys. Rev. B **84**, 014521 (2011); **84**, 115117 (2011).
[32]J. Guo, S. Jin, G. Wang, S. Wang, K. Zhu, T. Zhou, M. He, and X. Chen, Phys. Rev. B **82**, 180520(R) (2010).
[33]T. Qian, X.-P. Wang, W.-C. Jin, P. Zhang, P. Richard, G. Xu, X. Dai, Z. Fang, J.-G. Guo, X.-L. Chen, and H. Ding, Phys. Rev. Lett. **106**, 187001 (2011).
[34]R. Yu, P. Goswami, Q. Si, P. Nikolic, and J.-X. Zhu, e-print arXiv:1103.3259.
[35]C. Fang, Y.-L. Wu, R. Thomale, B. A. Bernevig, and J. Hu, Phys. Rev. X **1**, 011009 (2011).
[36]I. I. Mazin, Phys. Rev. B **84**, 024529 (2011).
[37]S. Maiti, M. M. Korshunov, T. A. Maier, P. J. Hirschfeld, and A. V. Chubukov, Phys. Rev. Lett. **107**, 147002 (2011).
[38]C. Cao, P. J. Hirschfeld, and H.-P. Cheng, Phys. Rev. B **77**, 220506(R) (2008).
[39]The 4×4 gap equations for s-wave and d-wave gaps are presented in the Supplementary Material of Ref. 37.
[40]C. Platt, R. Thomale, C. Honerkamp, S-C. Zhang, and W. Hanke, e-print arXiv:1106.5964.
[41]T. Sato, K. Nakayama, Y. Sekiba, P. Richard, Y.-M. Xu, S. Souma, T. Takahashi, G. F. Chen, J. L. Luo, N. L. Wang, and H. Ding, Phys. Rev. Lett. **103**, 047002 (2009); T. Terashima, M. Kimata, N. Kurita, H. Satsukawa, A. Harada, K. Hazama, M. Imai, A. Sato, K. Kihou, C. Lee, H. Kito, H. Eisaki, A. Iyo, T. Saito, H. Fukazawa, Y. Kohori, H. Harima, and S. Uji, J. Phys. Soc. Jpn. **79**, 053702 (2010).
[42]J. K. Dong, S. Y. Zhou, T. Y. Guan, H. Zhang, Y. F. Dai, X. Qiu, X. F. Wang, Y. He, X. H. Chen, and S. Y. Li, Phys. Rev. Lett. **104**, 087005 (2010); K. Hashimoto, A. Serafin, S. Tonegawa, R. Katsumata, R. Okazaki, T. Saito, H. Fukazawa, Y. Kohori, K. Kihou, C. H. Lee, A. Iyo, H. Eisaki, H. Ikeda, Y. Matsuda, A. Carrington, and T. Shibauchi, Phys. Rev. B **82**, 014526 (2010).
[43]C. H. Lee, K. Kihou, H. Kawano-Furukawa, T. Saito, A. Iyo, H. Eisaki, H. Fukazawa, Y. Kohori, K. Suzuki, H. Usui, K. Kuroki, and K. Yamada, Phys. Rev. Lett. **106**, 067003 (2011).
[44]A. V. Chubukov, M. G. Vavilov, and A. B. Vorontsov, Phys. Rev. B **80**, 140515(R) (2009).
[45]Y. Ran, F. Wang, H. Zhai, A. Vishwanath, and D.-H. Lee, Phys. Rev. B **79**, 014505 (2009).